GRAVITATIONAL LENSING

LECTURE 25

Docente: Massimo Meneghetti

AA 2016-2017

LUMINOUS AND DARK MATTER IN ETGS AND CLUSTERS FROM SL

- do ETGs and clusters live in dark matter halos?
- what is the relative spatial distribution of dark and luminous matter?
- what is the density profile of ETGs and clusters
- what is the nature of DM?
  - are DM density profiles universal?
  - how many substructures do DM halos contain?
  - are the halo shapes consistent with the collision-less picture of DM?

Good reading:

Treu, 2010, Ann. Rev. Astron. & Astrophys., 48, 87

Weinberg et al., 2015, PNAS, 112, 40

DO ETGS AND CLUSTERS LIVE IN DARK MATTER HALOS?

- a much larger amount of matter than the visible one is necessary to explain the observed SL effects.
- the mass inside the Einstein radius is very well determined and can be compared to the stellar mass
- the stellar mass can be derived from photometry and spectra:
  - assume an initial mass function (IMF)
  - apply stellar population synthesis models (SPS) to the photometric or to the spectroscopic data
  - obtain the stellar mass
- the total mass exceeds the stellar mass

WHAT IS THE RELATIVE SPATIAL DISTRIBUTION OF LUMINOUS AND DARK MATTER?

- baryons tend to condense inside halos to form stars
- by condensing to the center of the potential well, they affect the distribution of DM (e.g. by adiabatic contraction)
- however, there are other processes to account for: feedback mechanisms leading to heating of the IGM, which make less efficient such condensation
- with lensing, we can try to understand these processes by measuring the fraction of total mass in DM within a fixed projected radius (a fraction of R_e)
- stellar masses measured as before

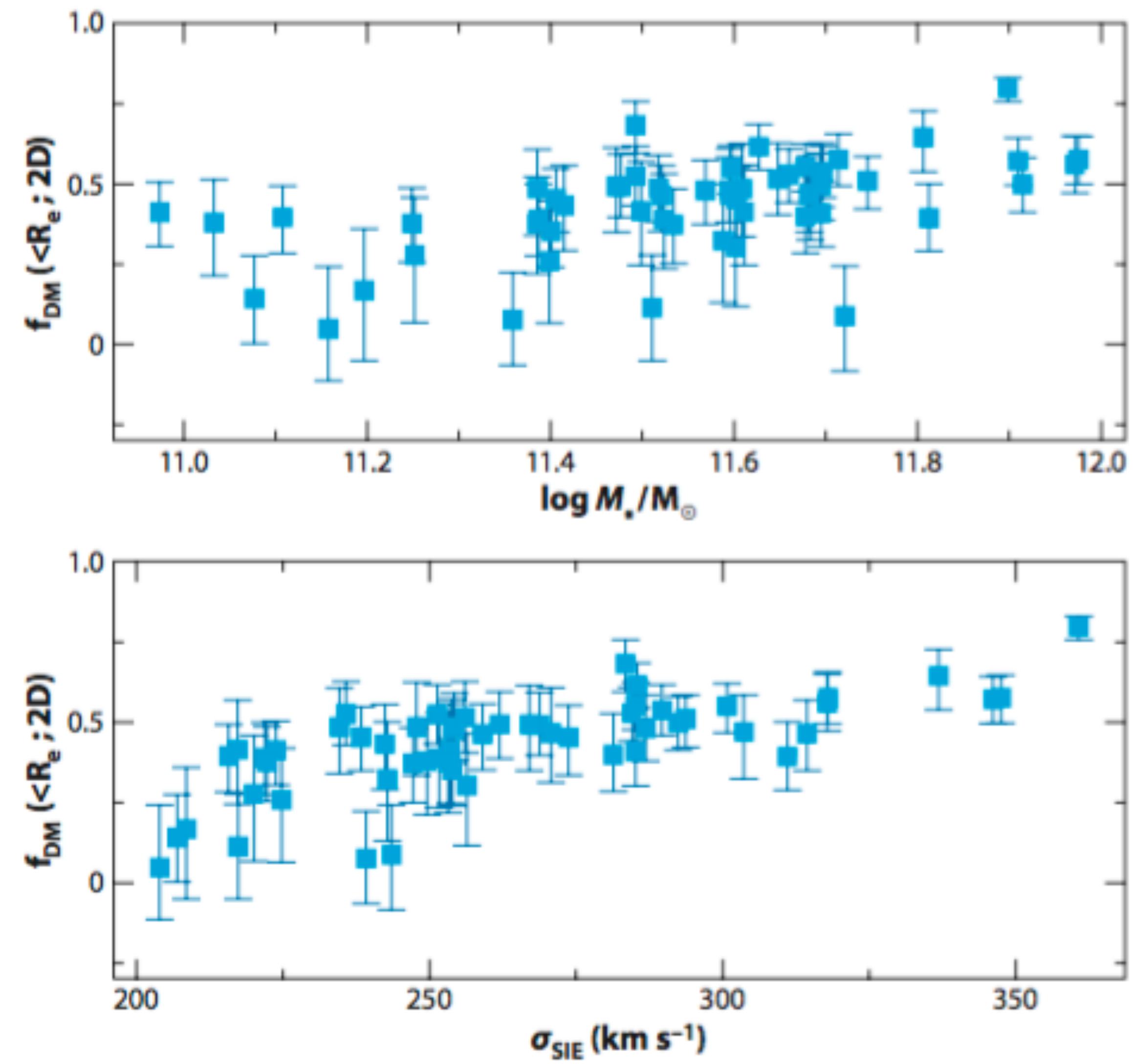

WHAT IS THE RELATIVE SPATIAL DISTRIBUTION OF LUMINOUS AND DARK MATTER?

From the virial theorem:

$$\sigma^2 \propto \frac{GM}{R} \qquad \Gamma = \frac{M}{L} \qquad L \propto IR^2$$

$$\sigma^2 \propto G\Gamma I R \qquad R_e = c\frac{\sigma^2}{GI_e\Gamma}$$

If c and M/L do not depend on mass, we expect the fundamental plane:

$$\log R_e = 2\log\sigma - \log I_e + d$$

Observationally:

$$\log R_e = a\log\sigma + b\log I_e + d' \qquad a = [1.1 \div 1.6] \qquad b = [-0.7 \div 0.8]$$

("tilt" of the fundamental plane)

WHAT IS THE RELATIVE SPATIAL DISTRIBUTION OF LUMINOUS AND DARK MATTER?

Lensing allows to measure the mass within a fraction of R_e! Thus we can use it to measure the "mass fundamental plane":

$$\sigma^2 \propto \frac{GM}{R} \qquad\qquad \log R_e = a_m \log \sigma + b_m \log \Sigma_e + d_m$$

It turns out that the mass fundamental plane is not tilted, indicating that the tilt of the fundamental plane is ascribable to a M/L which is not constant because of the increase in f_{DM} with mass (Bolton et al. 2008 using 53 ETGs from SLAC)

Bolton et al. (2008) also find that the mass distribution of these lenses is not consistent with the assumption that light traces mass.

MASS DENSITY PROFILES

Koopmans & Treu 2002, Treu & Koopmans 2002, Koopmans et al. 2006, 2009, Sonnenfeld et al. 2013, Spiniello et al. 2015

- Since 2005 (LSD survey; Koopmans & Treu), SL and stellar kinematics have been used to probe the mass profiles of ETGs
- Results point into the direction that, at the scales probed by these two methods, the total mass profiles are nearly isothermal
- there seems to be very little evolution with redshift

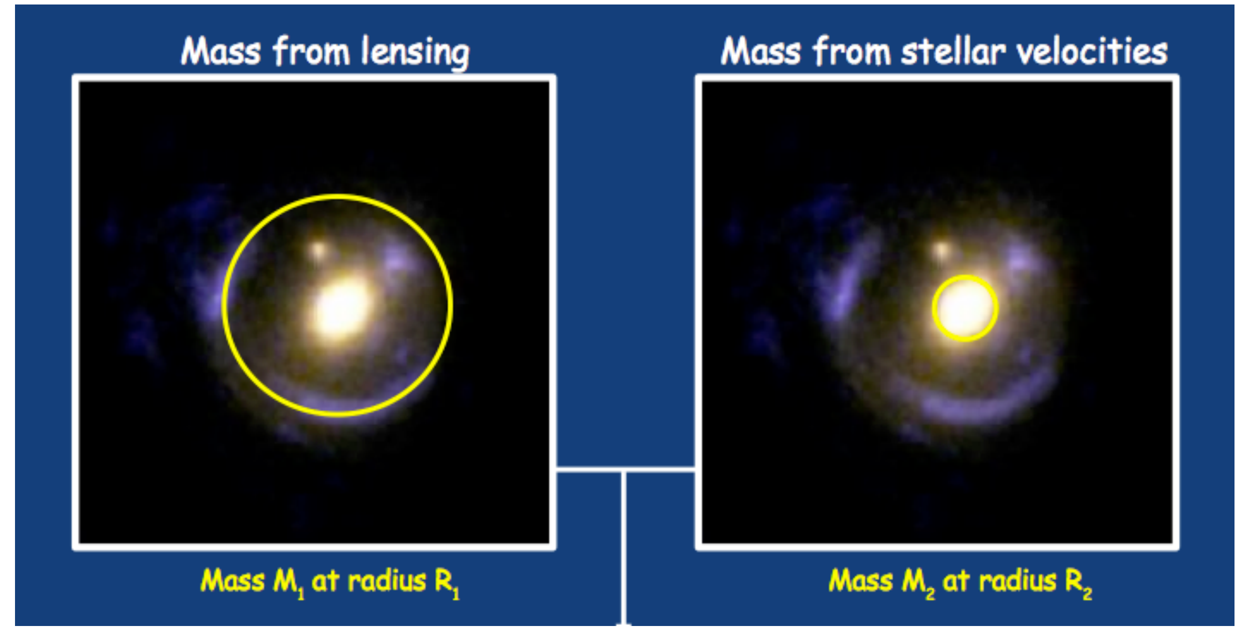

MASS DENSITY PROFILES

Koopmans & Treu 2002, Treu & Koopmans 2002, Koopmans et al. 2006, 2009, Sonnenfeld et al. 2013, Spiniello et al. 2015

- Since 2005 (LSD survey; Koopmans & Treu), SL and stellar kinematics have been used to probe the mass profiles of ETGs
- Results point into the direction that, at the scales probed by these two methods, the total mass profiles are nearly isothermal
- there seems to be very little evolution with redshift

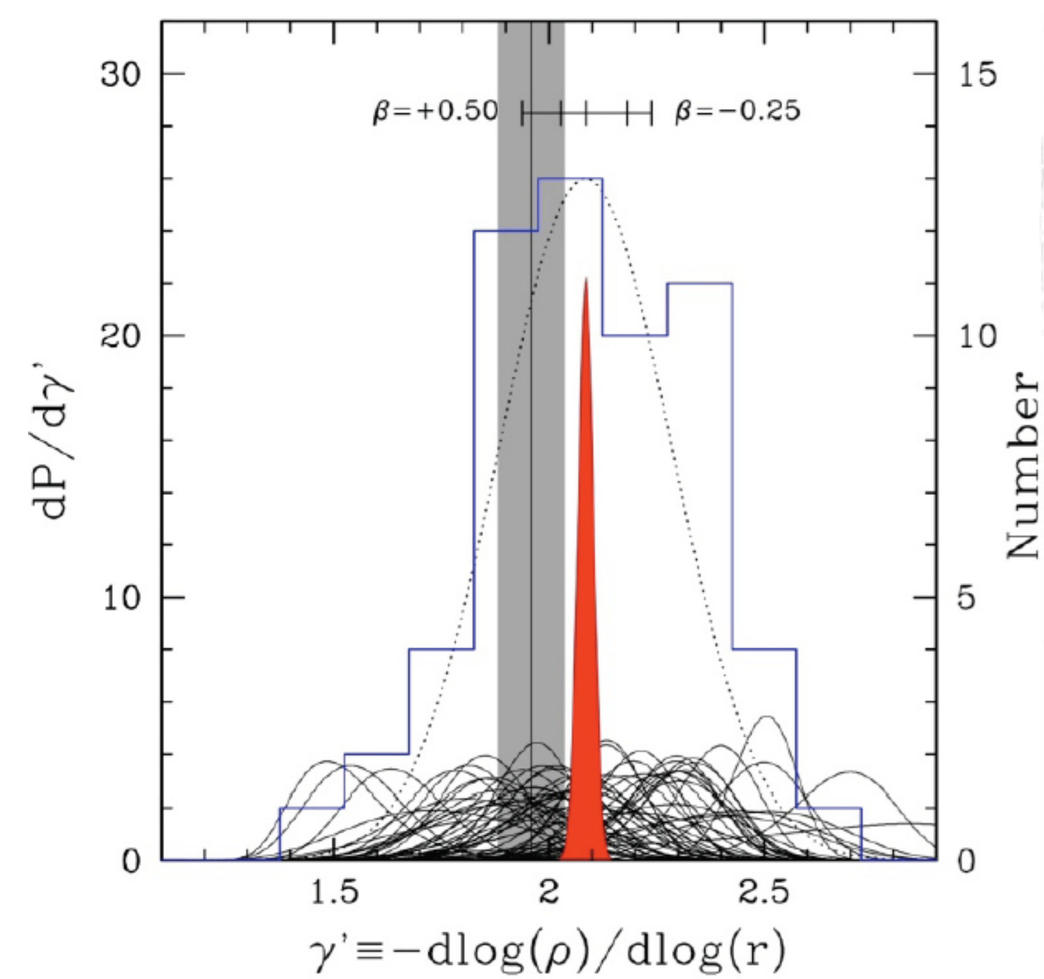

MASS DENSITY PROFILES

Koopmans & Treu 2002, Treu & Koopmans 2002, Koopmans et al. 2006, 2009, Sonnenfeld et al. 2013, Spiniello et al. 2015

- Since 2005 (LSD survey; Koopmans & Treu), SL and stellar kinematics have been used to probe the mass profiles of ETGs
- Results point into the direction that, at the scales probed by these two methods, the total mass profiles are nearly isothermal
- there seems to be very little evolution with redshift

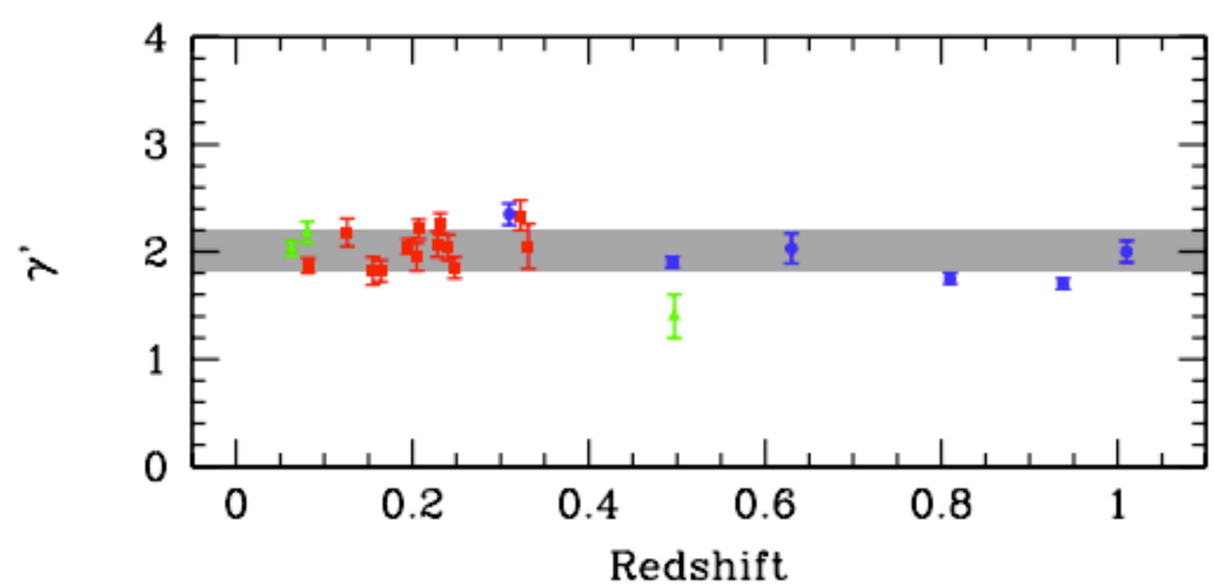

MASS DENSITY PROFILES

- In some rare cases, lensing alone may be sufficient to measure a slope
- this is the case of the so called "compound lenses" (Gavazzi et al. 2008)
- in such cases, two measurements of the mass at two different radii are possible, enabling the measurement of the slope of the mass profile
- the complication: it is a double lens!

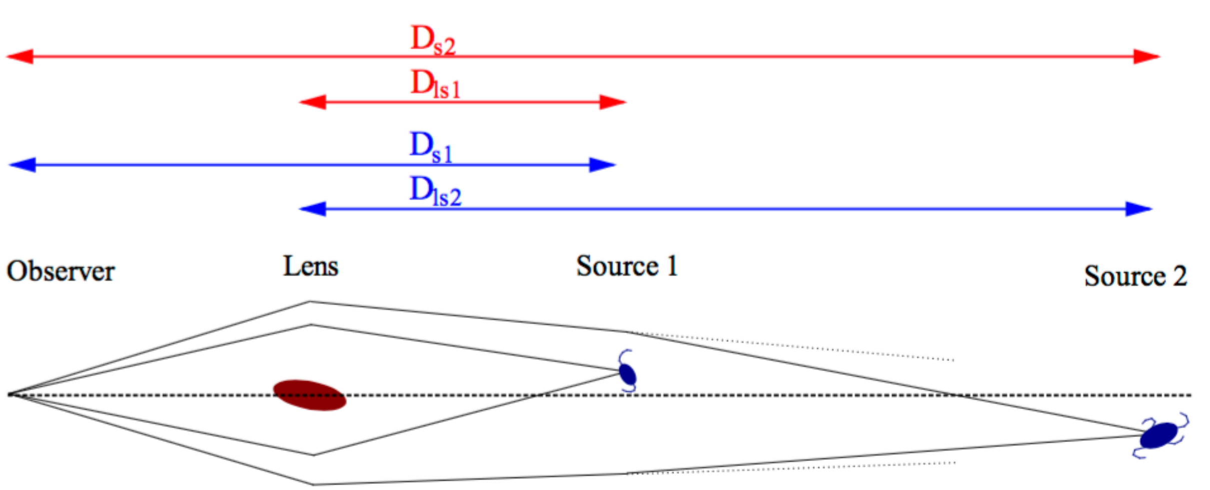

Collett et al. 2014

SDSSJ0946 + 1006

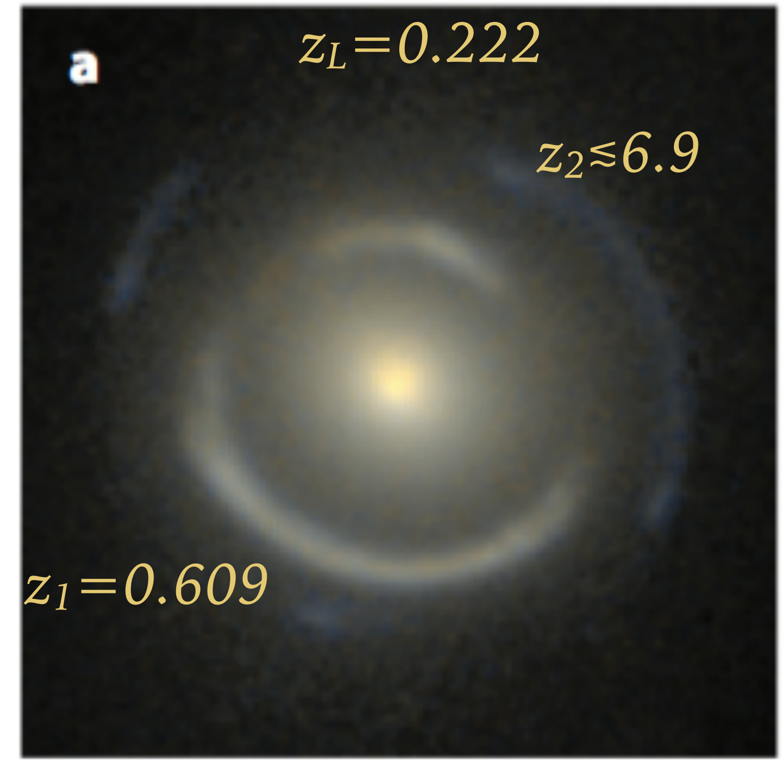

Double Einstein ring J0946 + 1006

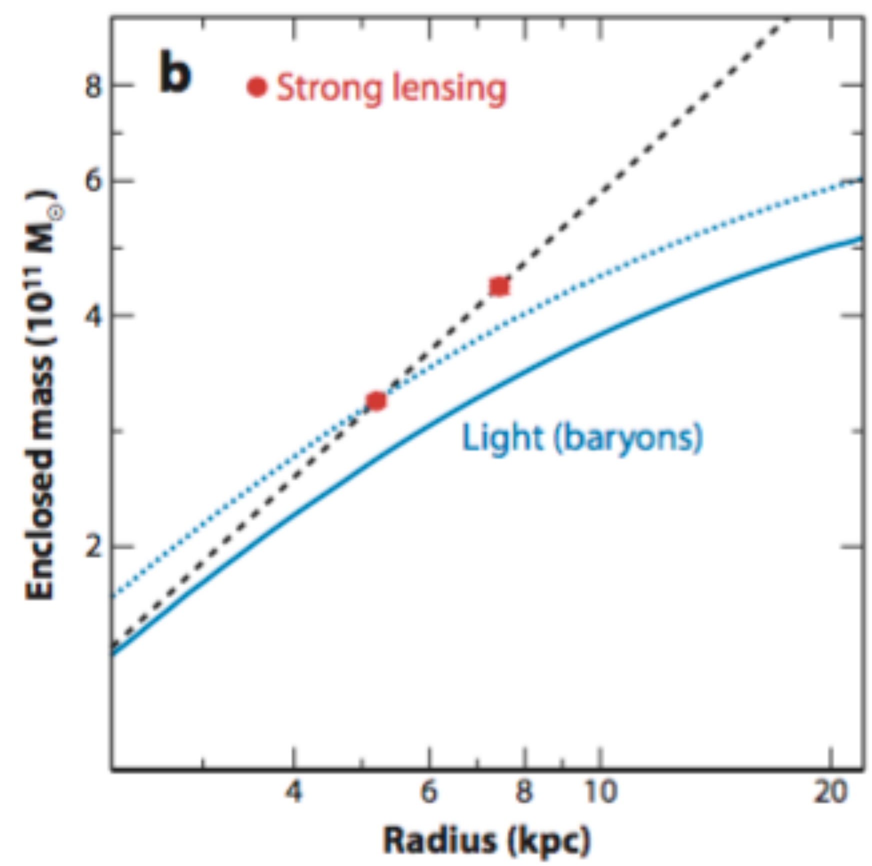

NFW

NAVARRO-FRENK-WHITE, 1997

- This profile was derived by fitting a large number of density profiles of DM halos in cosmological simulations
- Numerical simulations can be used to study the formation of the cosmic structures starting from suitable initial conditions
- The original work of NFW was based on pure N-body, collision less simulations.

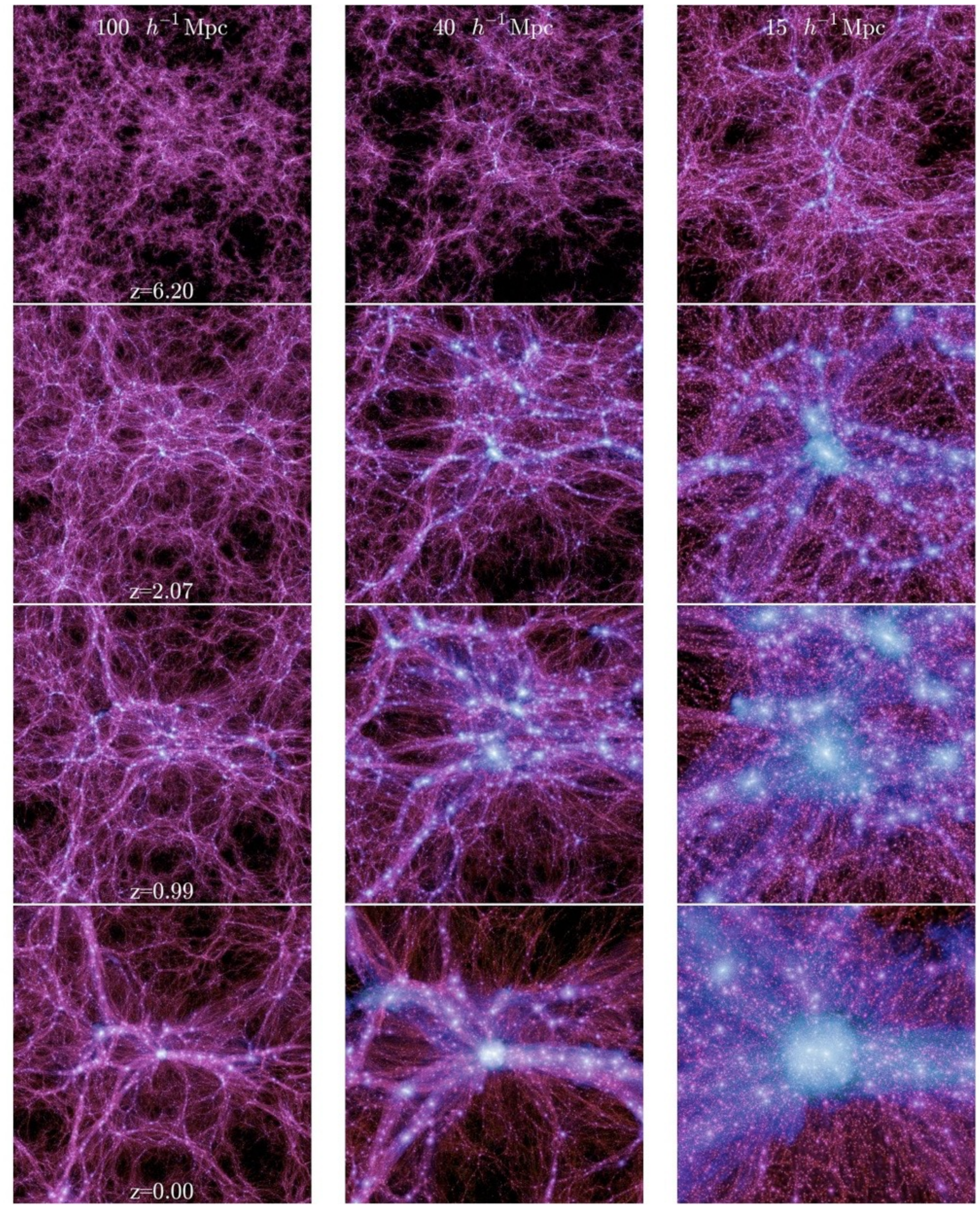

NFW

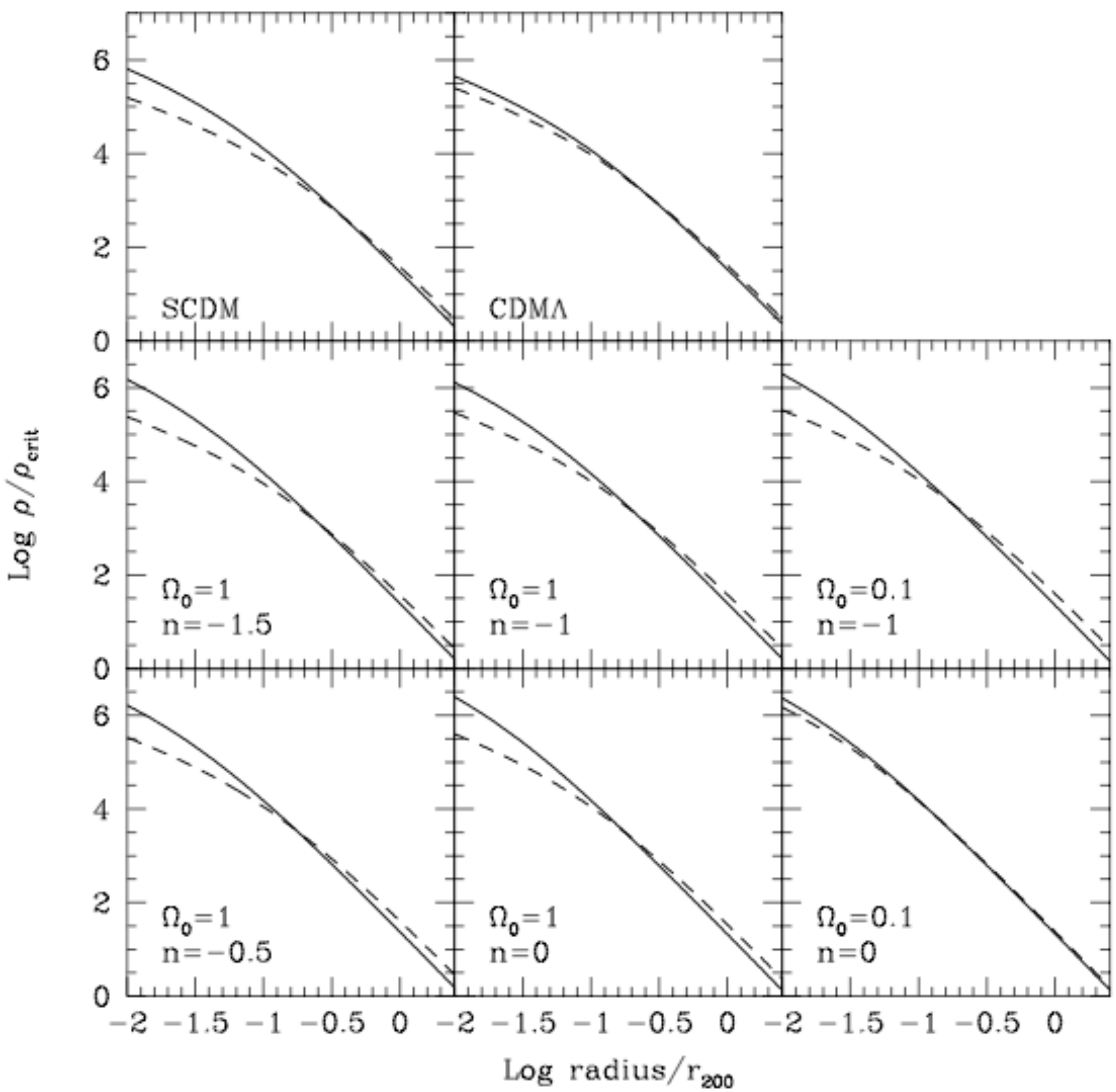

$$\rho(r) = \frac{\rho_s}{(r/r_s)(1 + r/r_s)^2}$$

$$r_{200} = 1.63 \times 10^{-2} \left(\frac{M_{200}}{h^{-1}M_\odot}\right)^{1/3} \left[\frac{\Omega_0}{\Omega(z)}\right]^{-1/3} (1+z)^{-1} h^{-1} \text{ kpc}$$

$$\rho_s = \frac{200}{3}\rho_{\rm cr}\frac{c^3}{[\ln(1+c) - c/(1+c)]}$$

$$c \equiv r_{200}/r_s$$

NFW VS COSMOLOGY

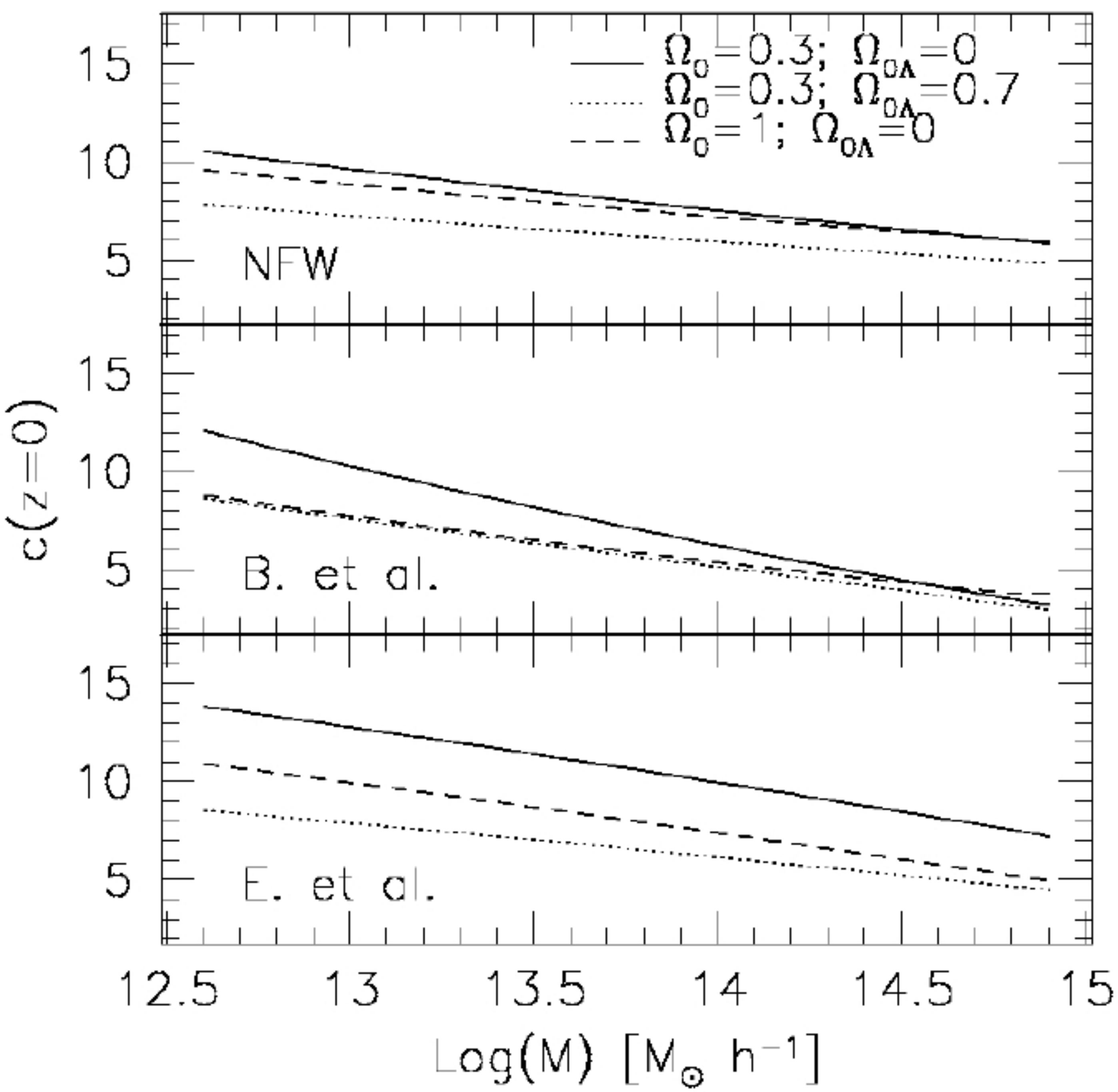

NFW LENSES

$$\rho(r) = \frac{\rho_s}{(r/r_s)(1+r/r_s)^2} \quad \Rightarrow \quad \xi_0 = r_s \quad \Rightarrow \quad \Sigma(x) = \frac{2\rho_s r_s}{x^2-1} f(x)$$

$$f(x) = \begin{cases} 1 - \frac{2}{\sqrt{x^2-1}} \operatorname{arctan}\sqrt{\frac{x-1}{x+1}} & (x > 1) \\ 1 - \frac{2}{\sqrt{1-x^2}} \operatorname{arctanh}\sqrt{\frac{1-x}{1+x}} & (x < 1) \\ 0 & (x = 1) \end{cases}$$

$$\Psi(x) = 4\kappa_s g(x) \qquad \kappa_s \equiv \rho_s r_s \Sigma_{\rm cr}^{-1}$$

$$g(x) = \frac{1}{2}\ln^2\frac{x}{2} + \begin{cases} 2\operatorname{arctan}^2\sqrt{\frac{x-1}{x+1}} & (x > 1) \\ -2\operatorname{arctanh}^2\sqrt{\frac{1-x}{1+x}} & (x < 1) \\ 0 & (x = 1) \end{cases}$$

$$\alpha(x) = \frac{4\kappa_s}{x} h(x)$$

$$h(x) = \ln\frac{x}{2} + \begin{cases} \frac{2}{\sqrt{x^2-1}} \operatorname{arctan}\sqrt{\frac{x-1}{x+1}} & (x > 1) \\ \frac{2}{\sqrt{1-x^2}} \operatorname{arctanh}\sqrt{\frac{1-x}{1+x}} & (x < 1) \\ 1 & (x = 1) \end{cases}$$

NFW VS SIS

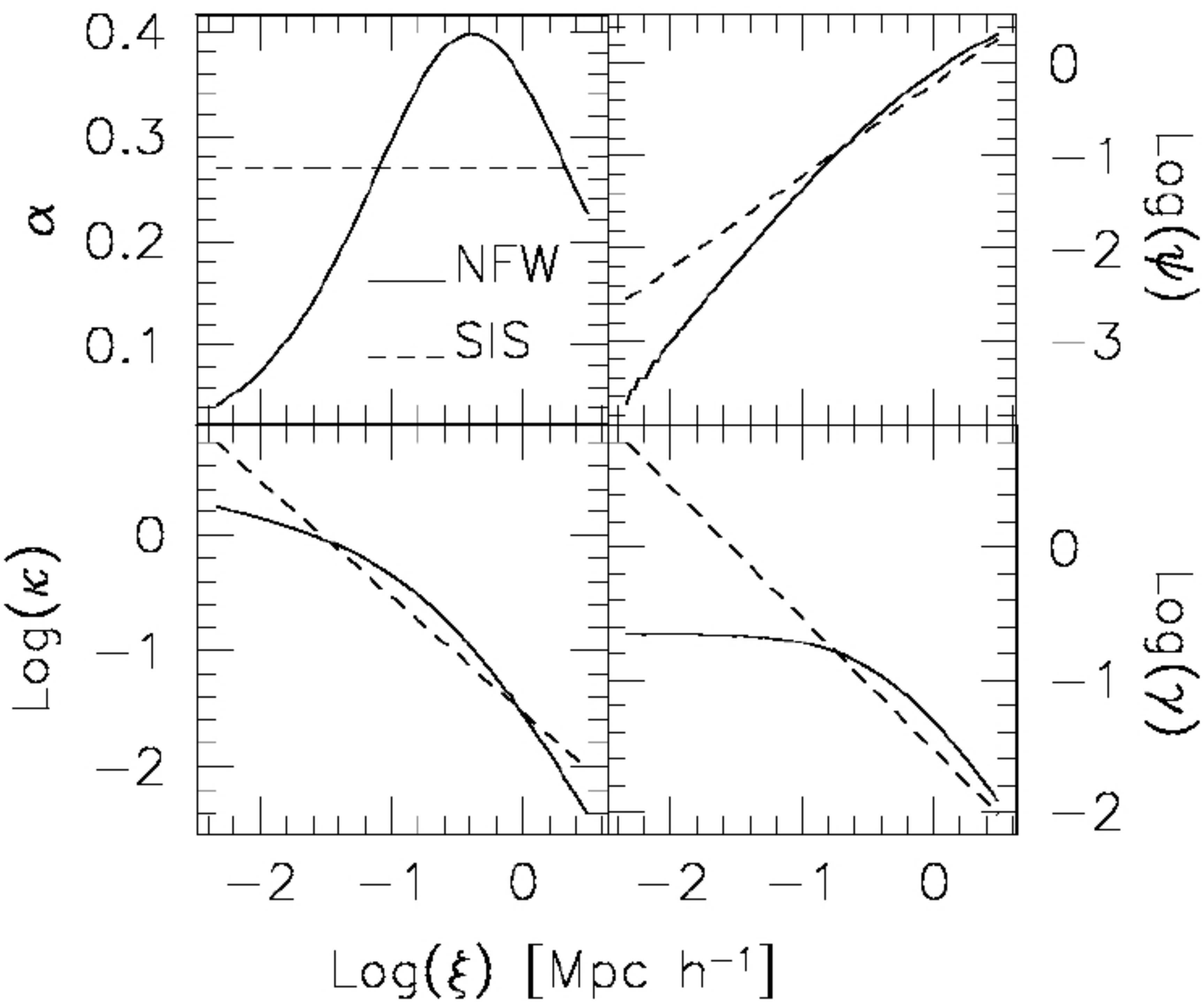

ARE DARK MATTER HALOS UNIVERSAL?

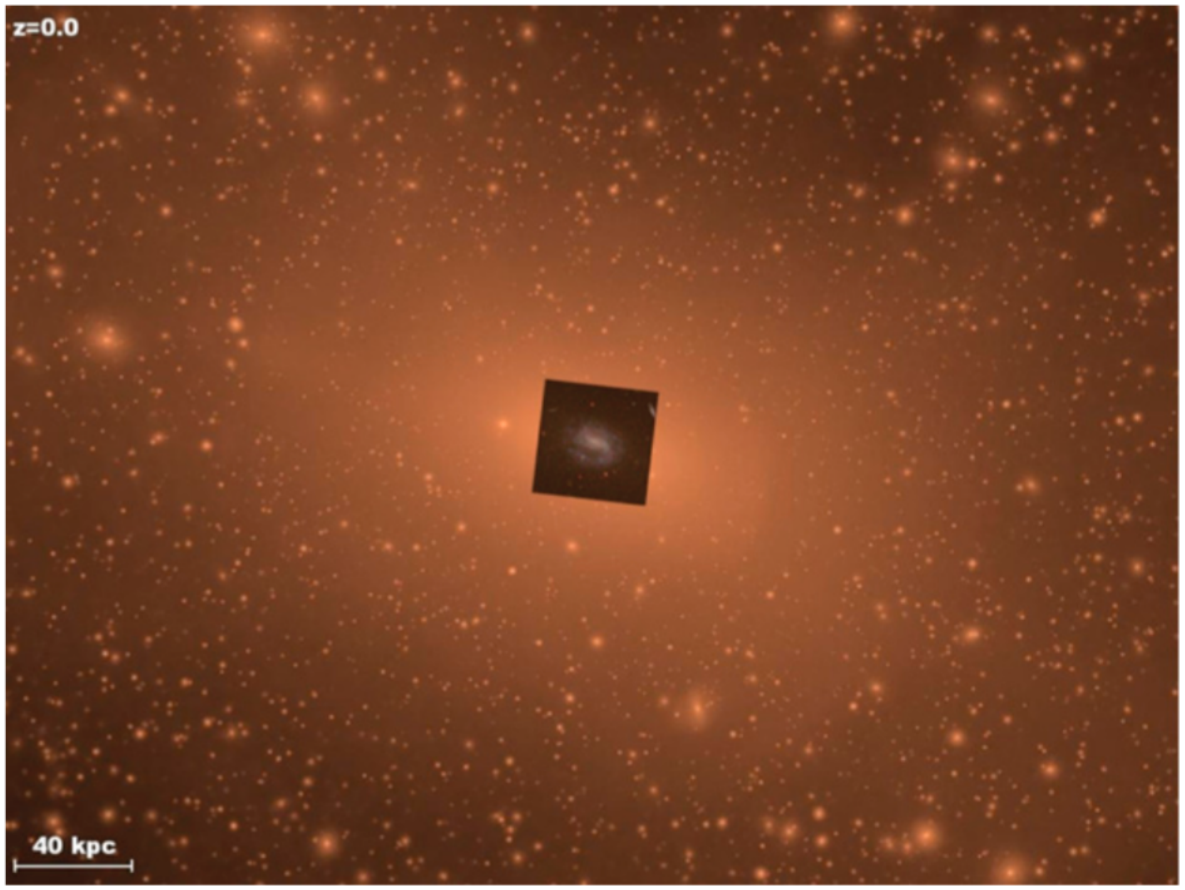

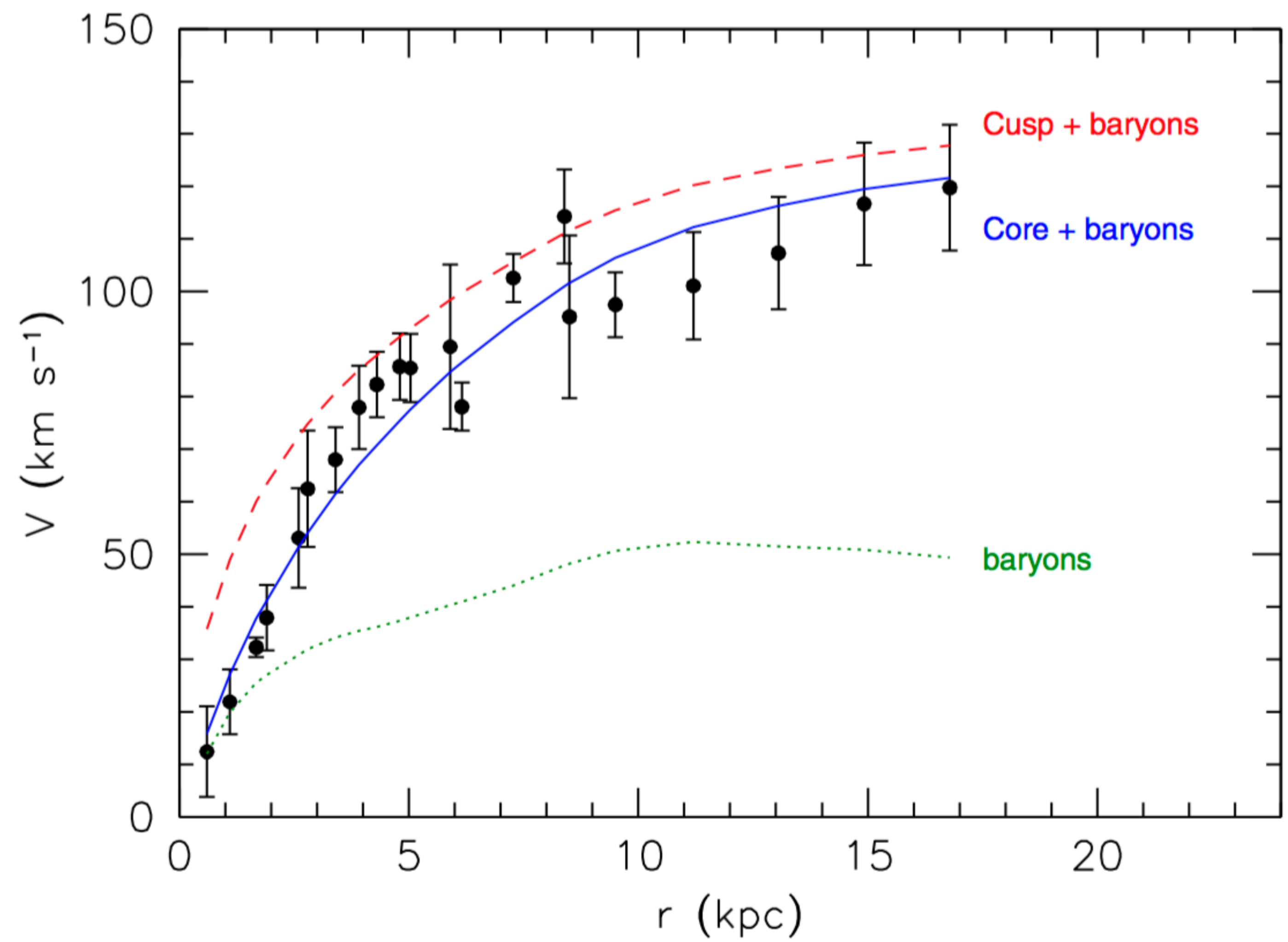

Weinberg et al. 2015

The cusp-core problem: *rotation curves of low-surface brightness galaxies (believed to be dark matter dominated) are inconsistent with cuspy dark-matter profiles (such as the NFW profiles). The circular velocity curve (dots with error-bars refer to the galaxy F568-3)*

SUBSTRUCTURES: THE MISSING SATELLITE AND “THE TOO BIG TO FAIL” PROBLEMS

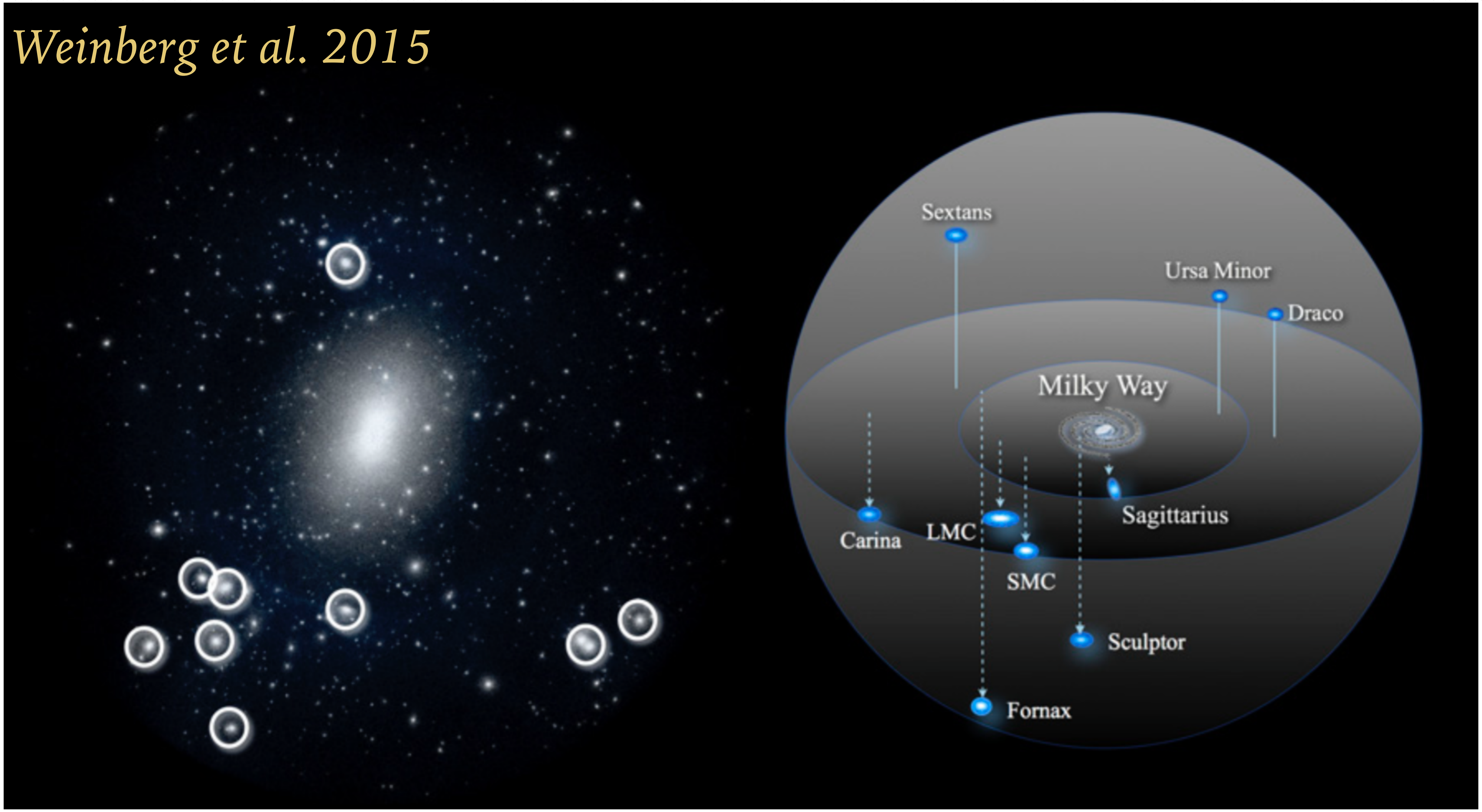

The missing-satellite problem: *simulations show that CDM forms many more sub-halos than observed around the Milky-Way*

SUBSTRUCTURES: THE MISSING SATELLITE AND "THE TOO BIG TO FAIL" PROBLEMS

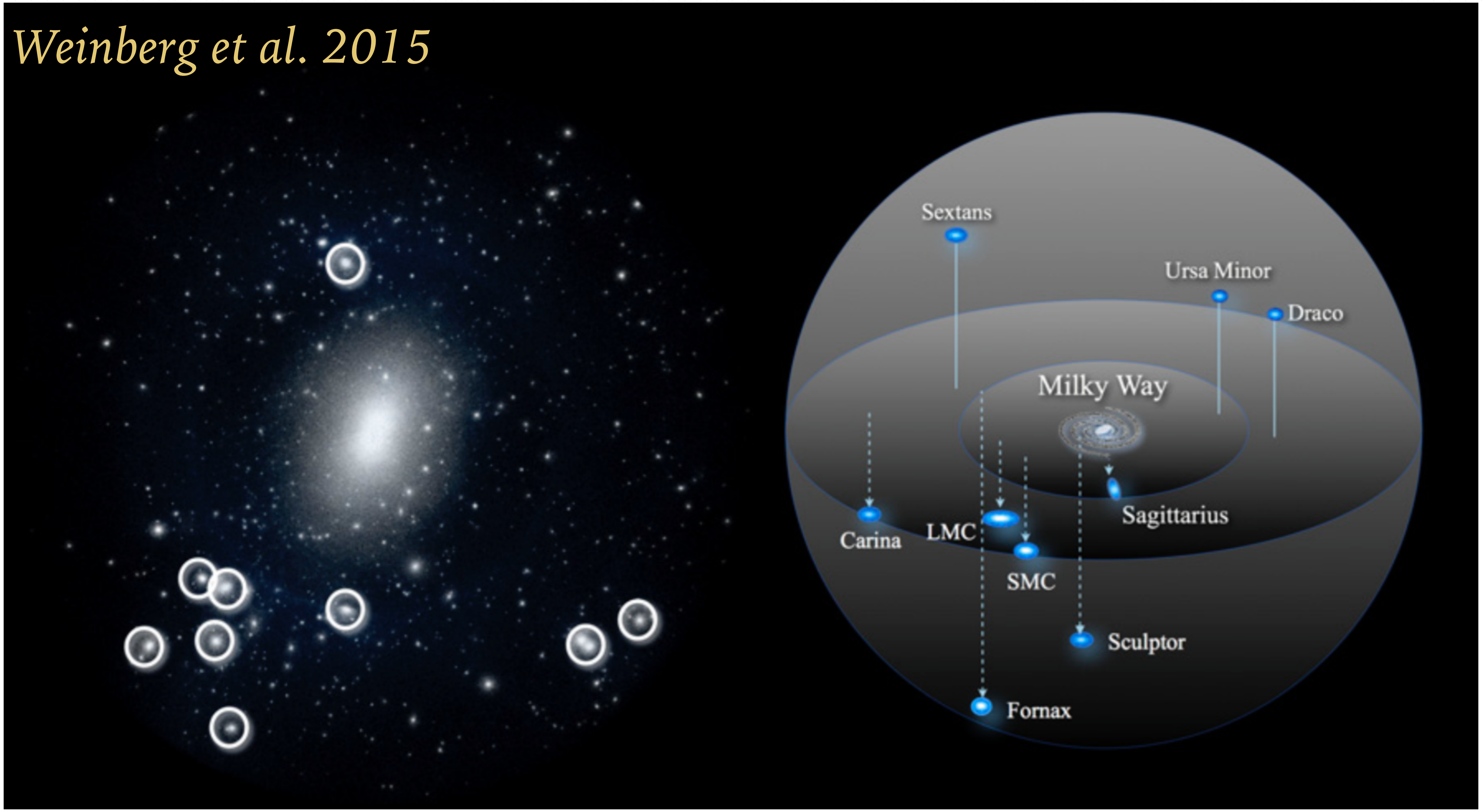

~~***The missing-satellite problem:*** *simulations show that CDM forms many more sub-halos than observed around the Milky Way*~~

The too-big-to-fail problem: *the biggest sub-halos in simulations are too massive and dense to host the observed dwarf-satellites (x5 in mass)!*

SUBSTRUCTURES: THE MISSING SATELLITE AND “THE TOO BIG TO FAIL” PROBLEMS

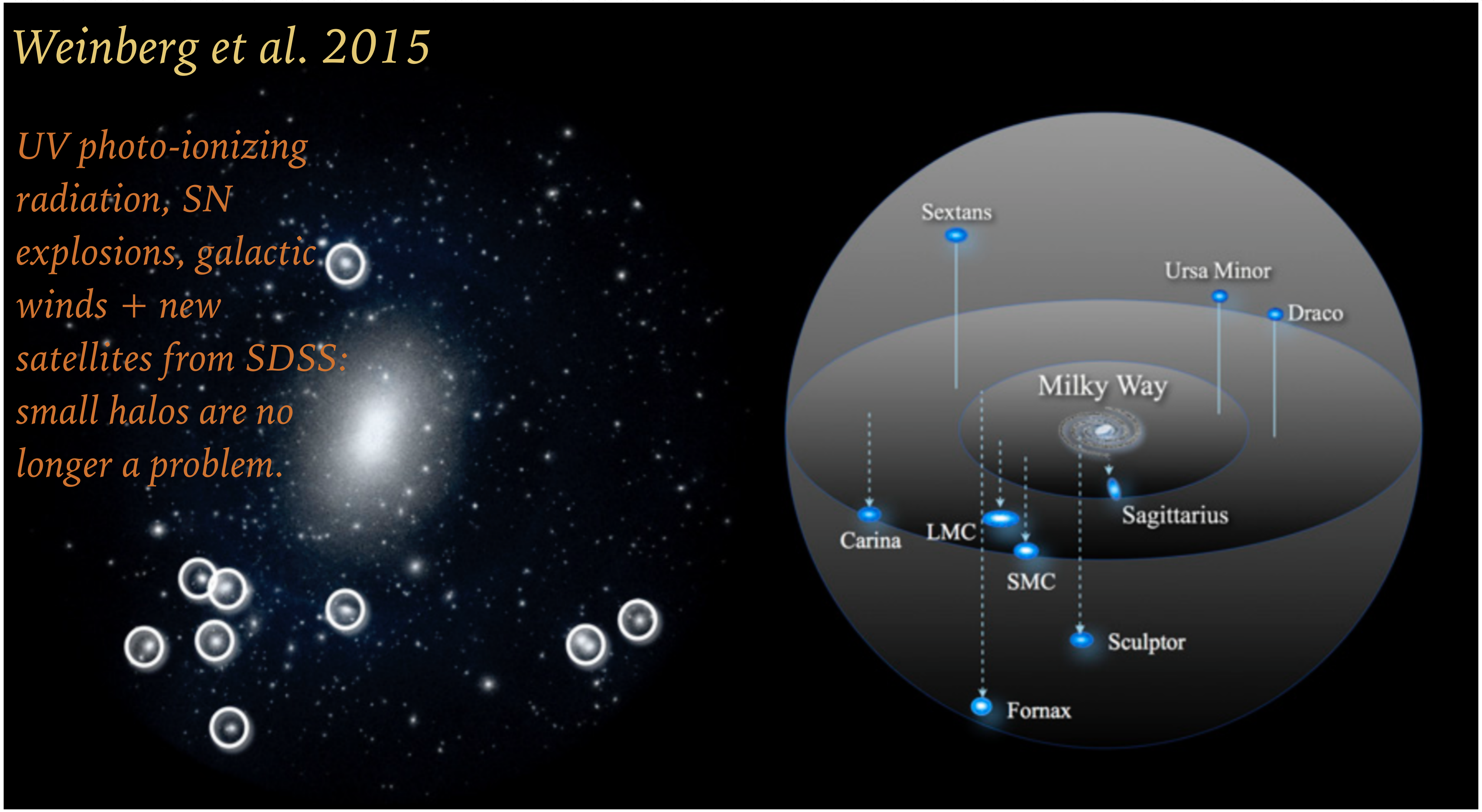

~~***The missing-satellite problem:*** *simulations show that CDM forms many more sub-halos than observed around the Milky Way*~~

The too-big-to-fail problem: *the biggest sub-halos in simulations are too massive and dense to host the observed dwarf-satellites (x5 in mass)!*

IS THE SOLUTION TO BE FOUND IN BARYONIC PHYSICS?

- The cusp-core and the too-big-to-fail problems both point to the same conclusion: dark matter halos have smaller central densities than expected from CDM
- The are "baryonic" solutions to this problem: feedback episodes from SNe or AGN can create potential instabilities which end up creating a core (Governato et al. 2012)
- Some results, however, seem to indicate that dwarf galaxies are cored (Ferrero et al. 2012)…

ARE DARK MATTER HALOS UNIVERSAL?

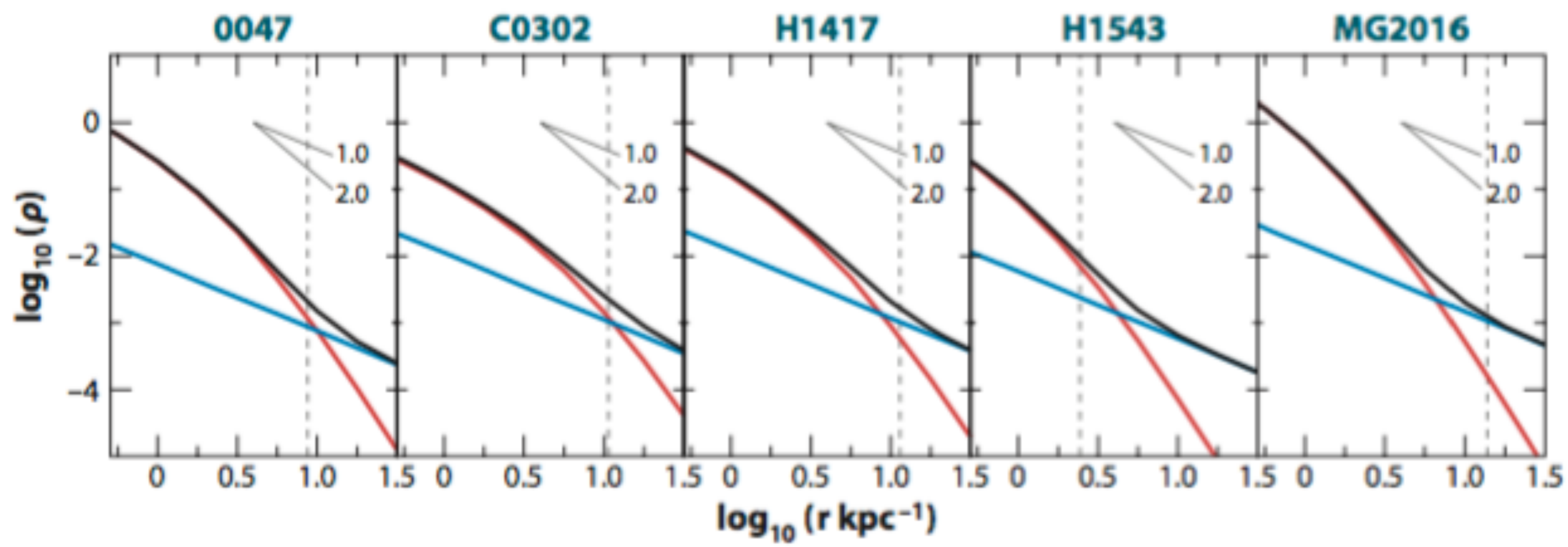

Difficult to say using SL by ETGs, because of the bulge-halo conspiracy…

However, imposing the slope of the NFW profile, the assumption of a universal IMF to derive the stellar masses doesn't work (SLACS, Treu et al. 2010).

ARE DARK MATTER HALOS UNIVERSAL?

Newman et al. 2012, 2013; see also Sand et al. 2005

On cluster scales: the combination of SL and stellar kinematics in some galaxy clusters seems to point towards profiles that are flatter than NFW on small scales (<30 kpc)

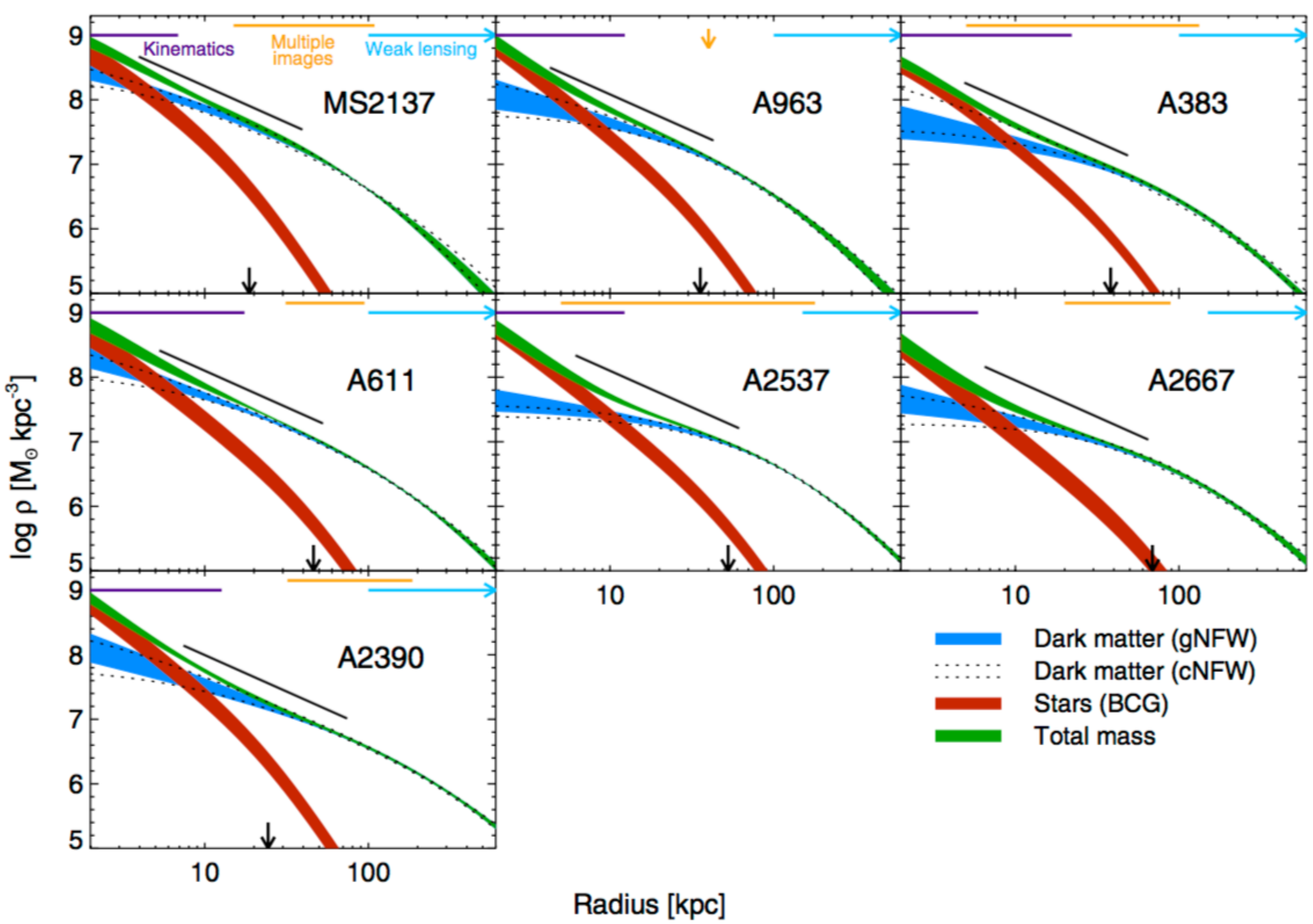

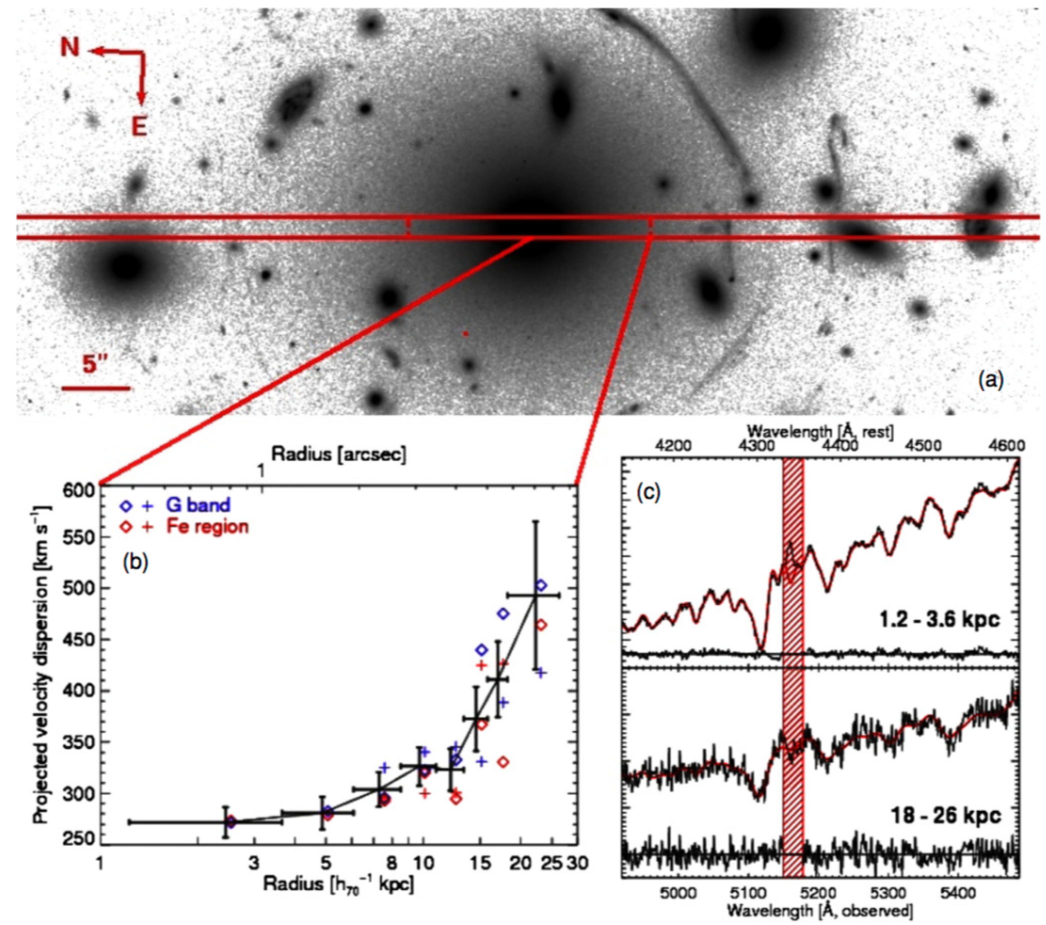

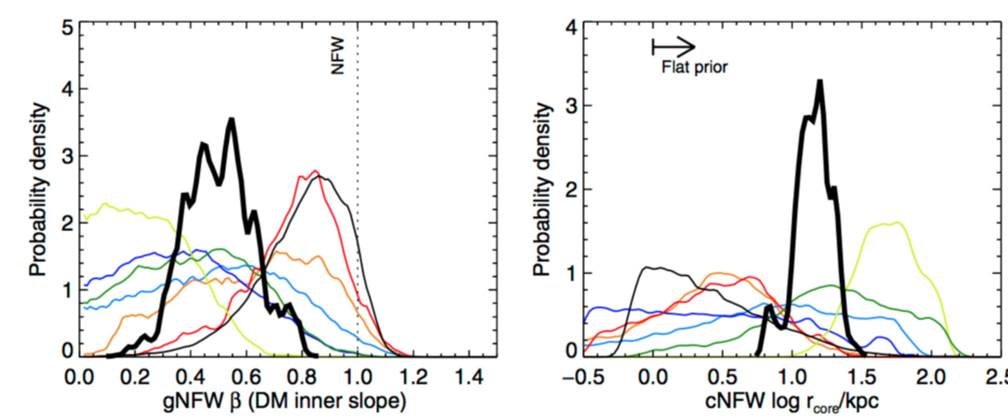

$$\rho_{\rm DM}(r) = \frac{\rho_s}{(r/r_s)^\beta (1+r/r_s)^{3-\beta}} \qquad \rho_{\rm DM}(r) = \frac{b\rho_s}{(1+br/r_s)(1+r/r_s)^2}.$$

ARE DARK MATTER HALOS UNIVERSAL?

Newman et al. 2015

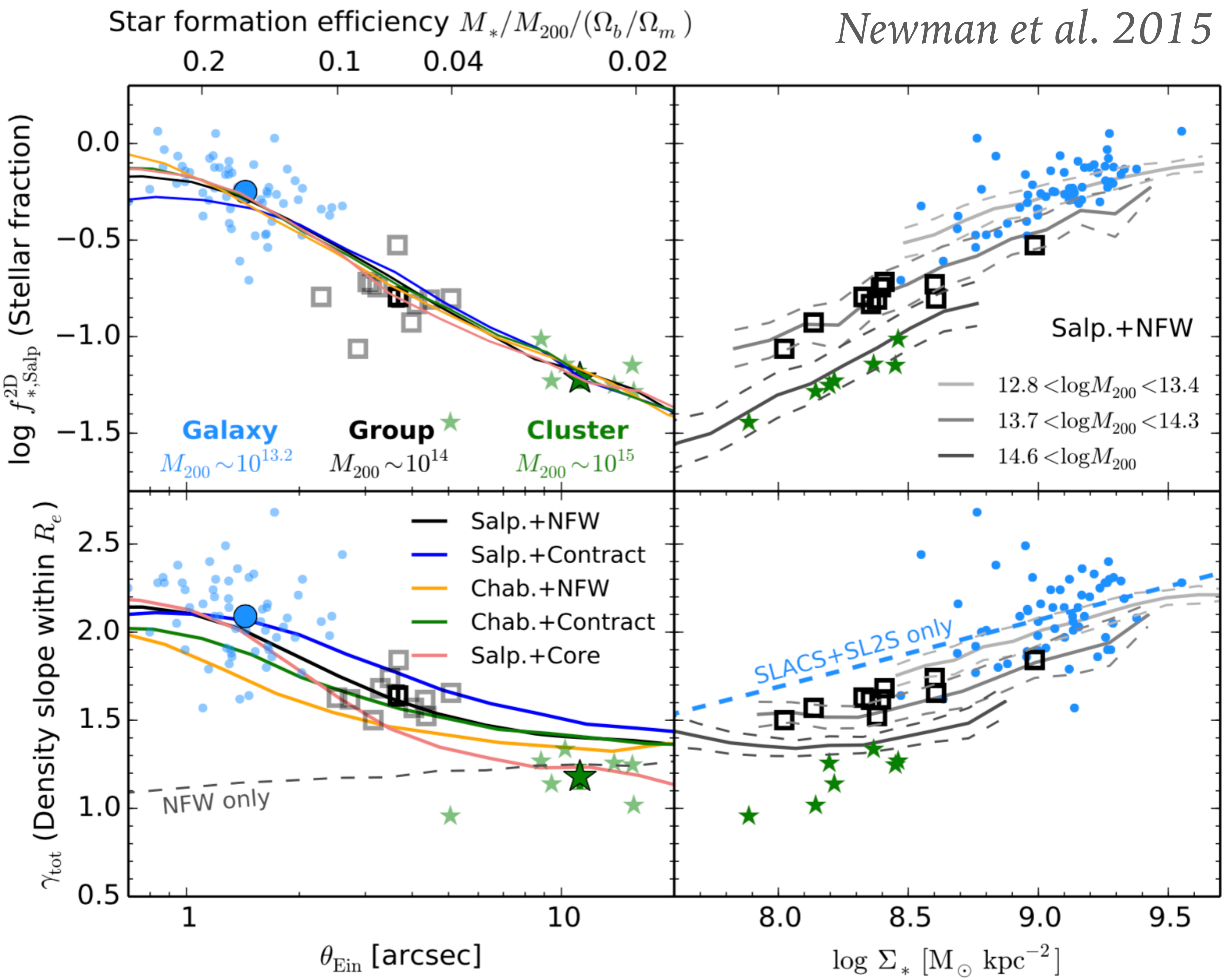

ARE DARK MATTER HALOS UNIVERSAL?

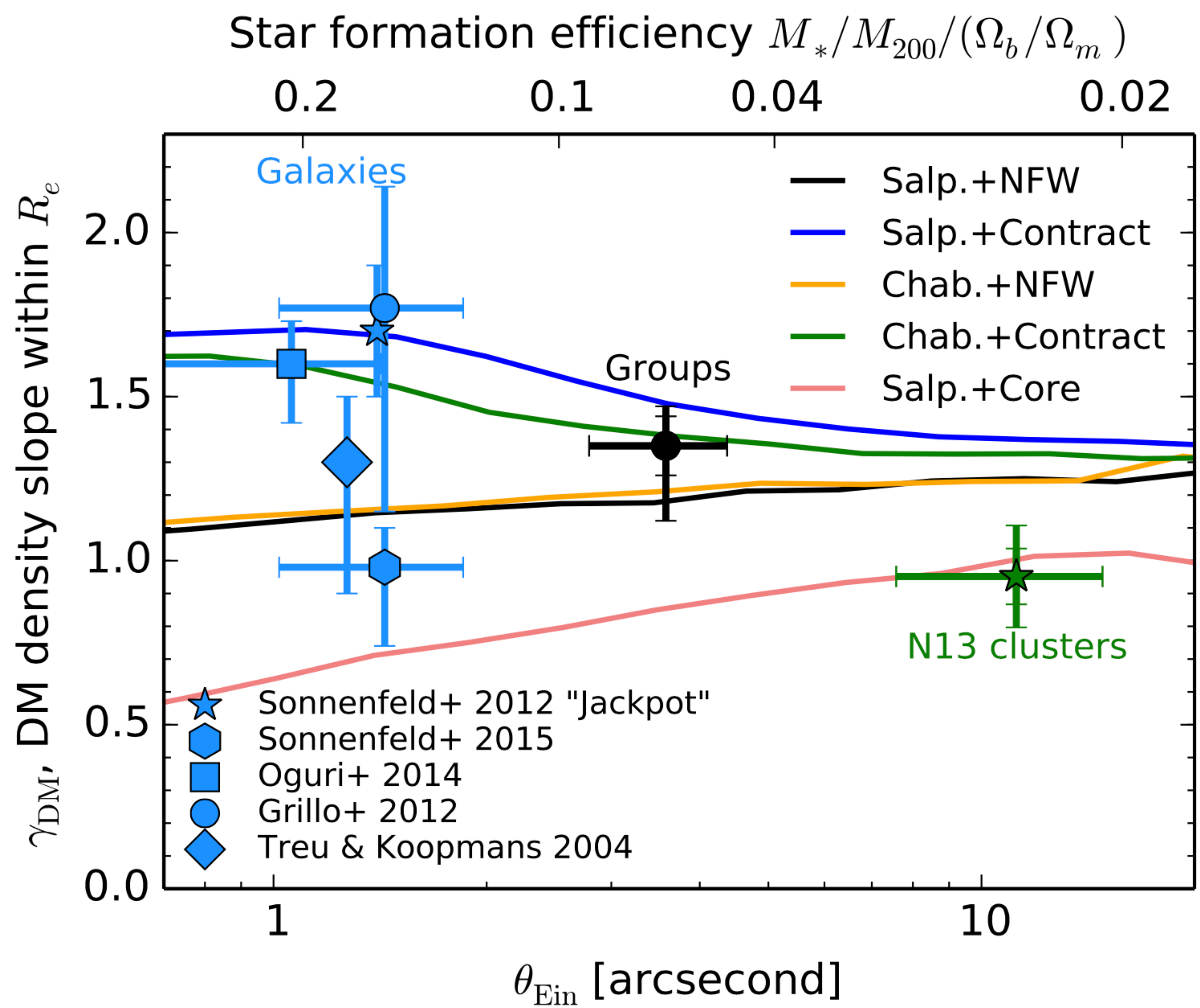

CAVEATS

- lensing probes the projected mass distribution rather than the three dimensional one
- stellar kinematics is affected by its own uncertainties (e.g. mass-anisotropy degeneracy, projection effects, etc)
- lensing is affected by mass-sheet degeneracy, which is not easy to break given the uncertainties on the stellar kinematics mass estimates.
- the IMF is affected by uncertainties too, and it is degenerate with the slope (but massive galaxies seem better described by Salpter IMF)

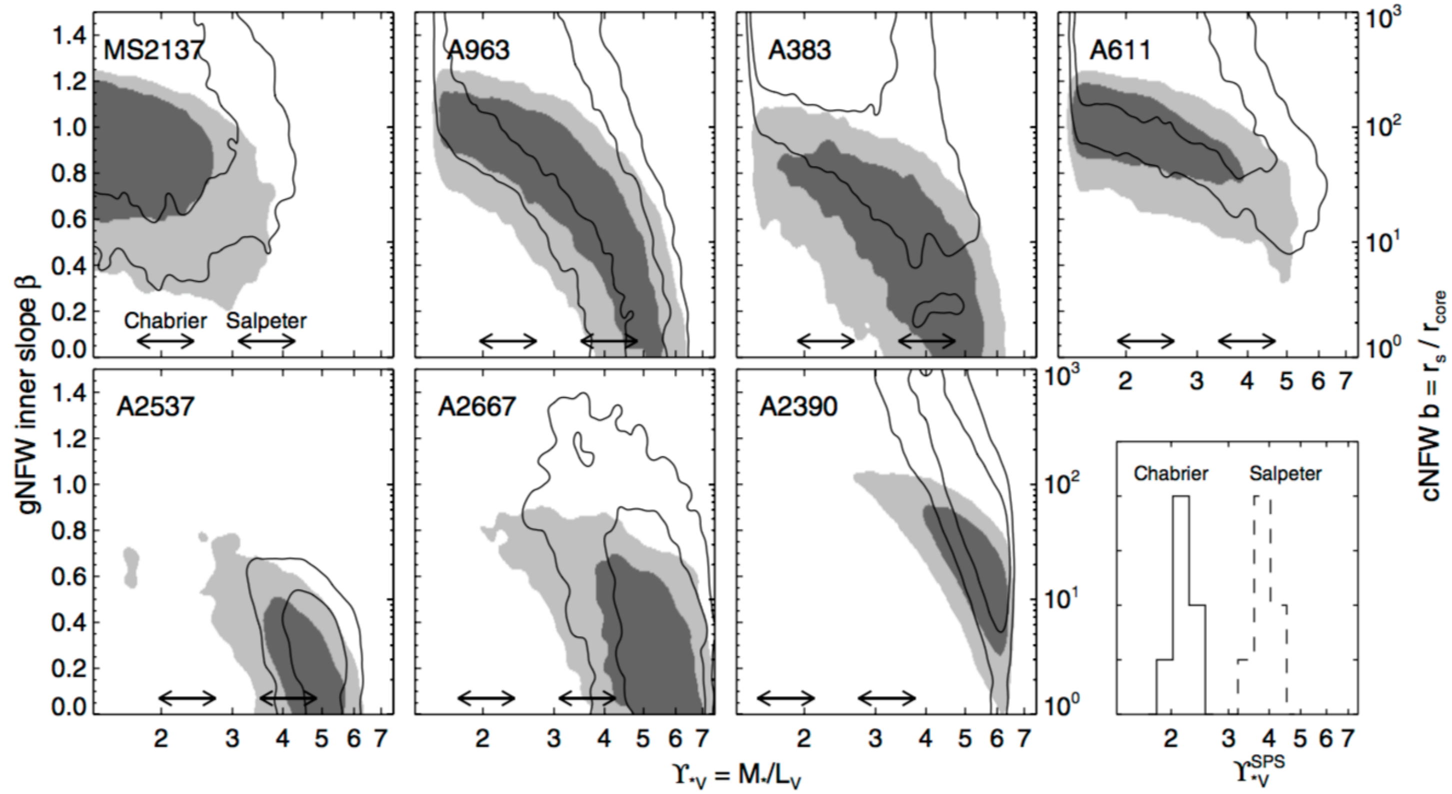

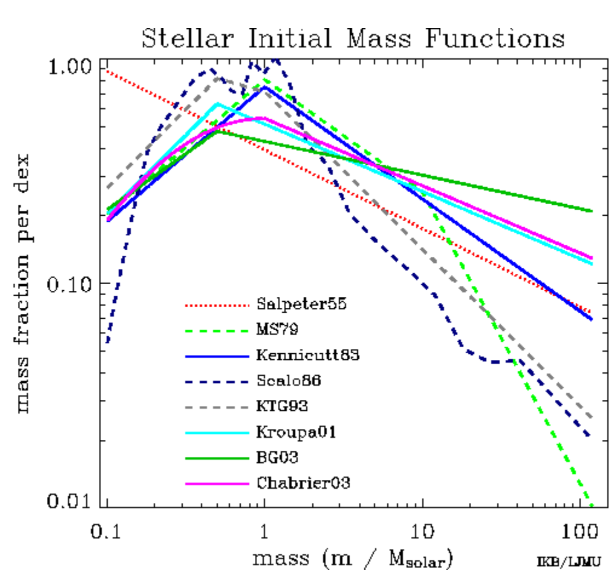

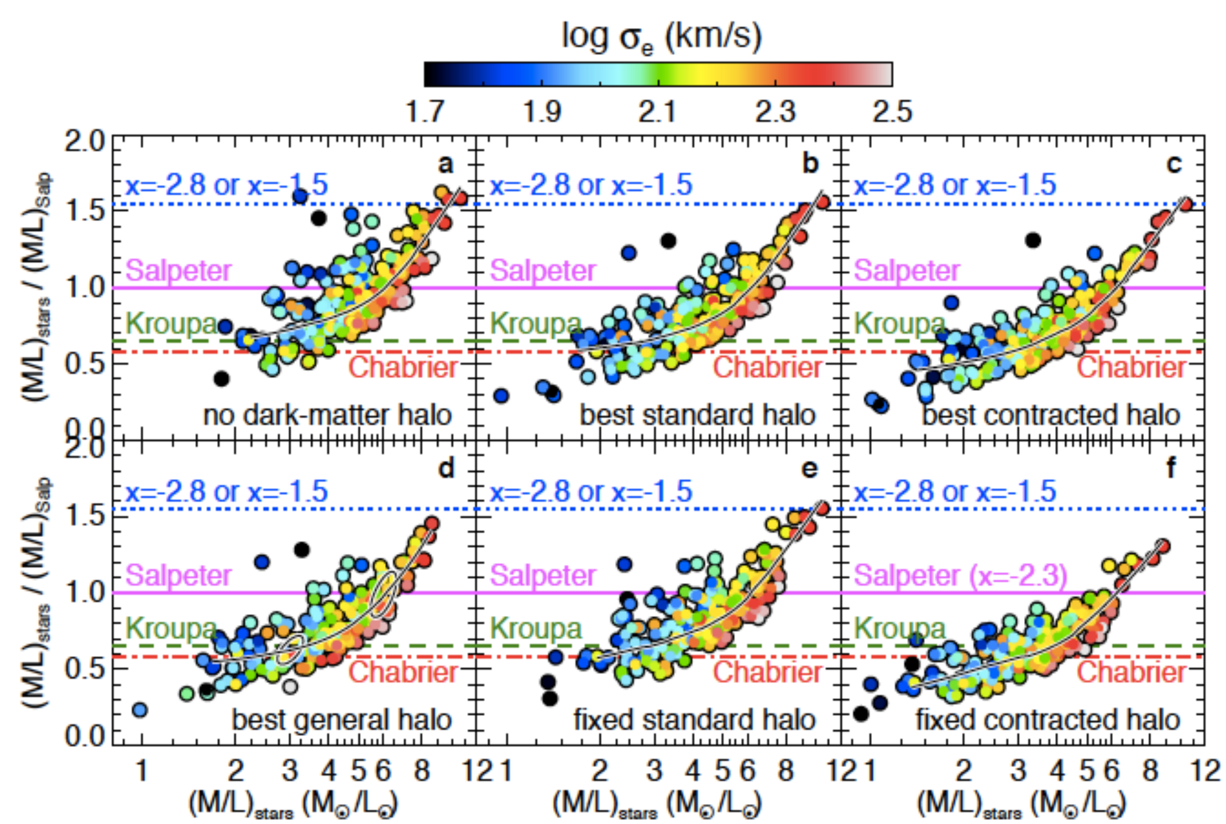

Cappellari et al 2012

WHAT IS THE NATURE OF DARK MATTER?

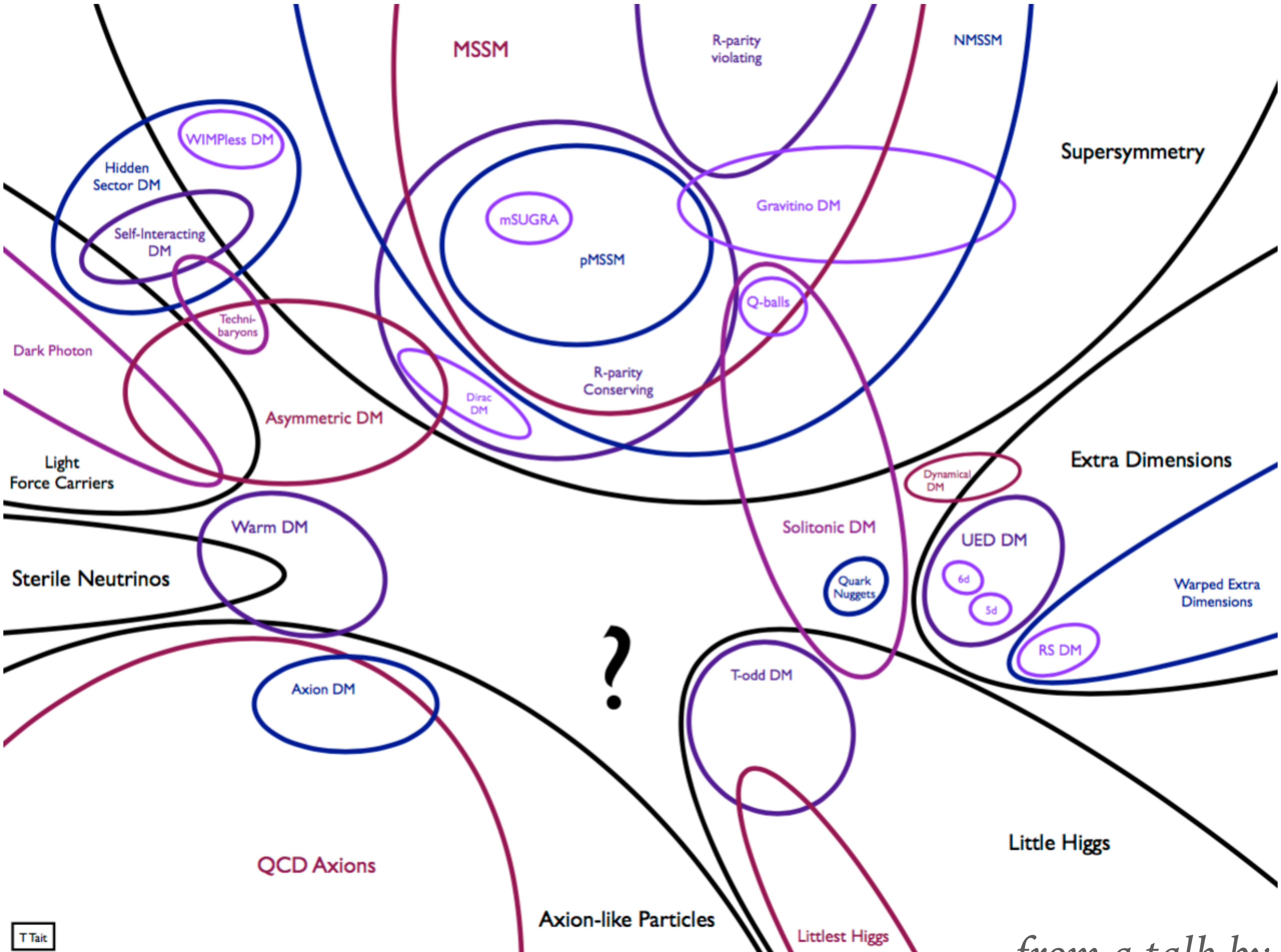

from a talk by T. Tait

IS THE NATURE OF DM INCONSISTENT WITH STANDARD CDM?

- Self-interacting dark matter? *Wherever density is large, self-interactions become important and erase the cusps (suppressing also the satellites)*
- Warm-dark-matter? *Free-streaming in the early universe suppresses small scales*
- ?

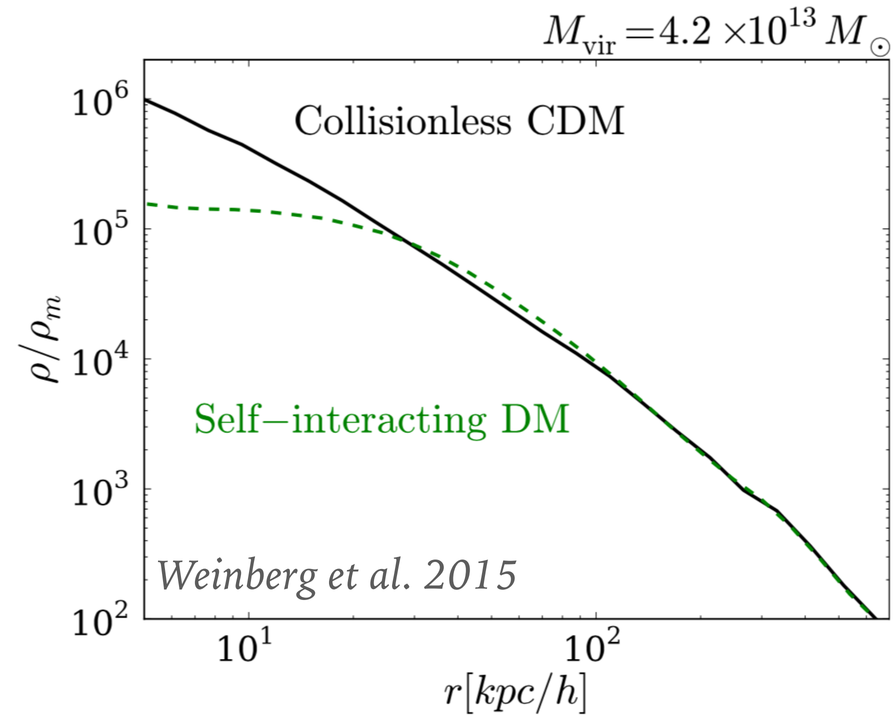

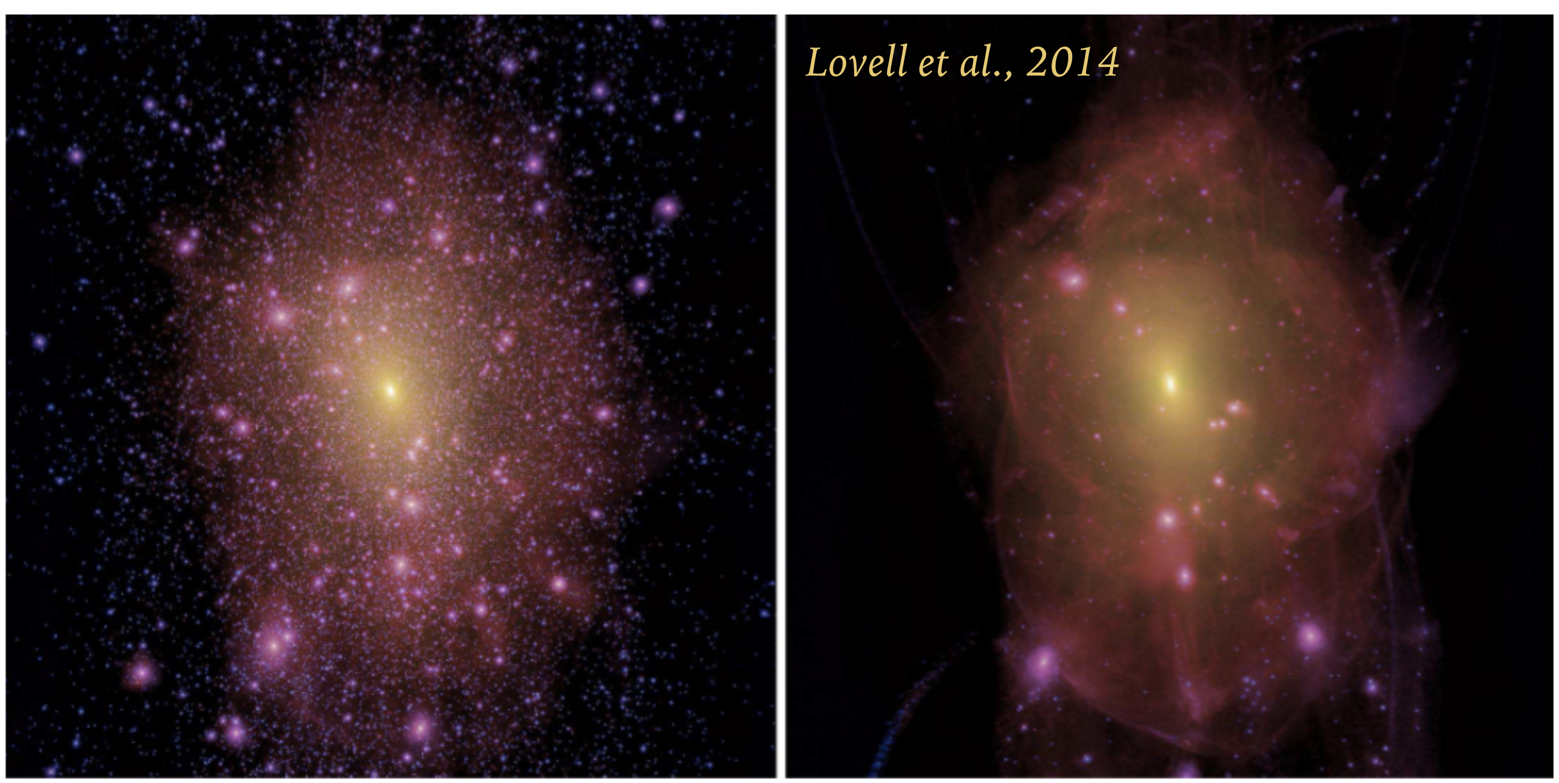

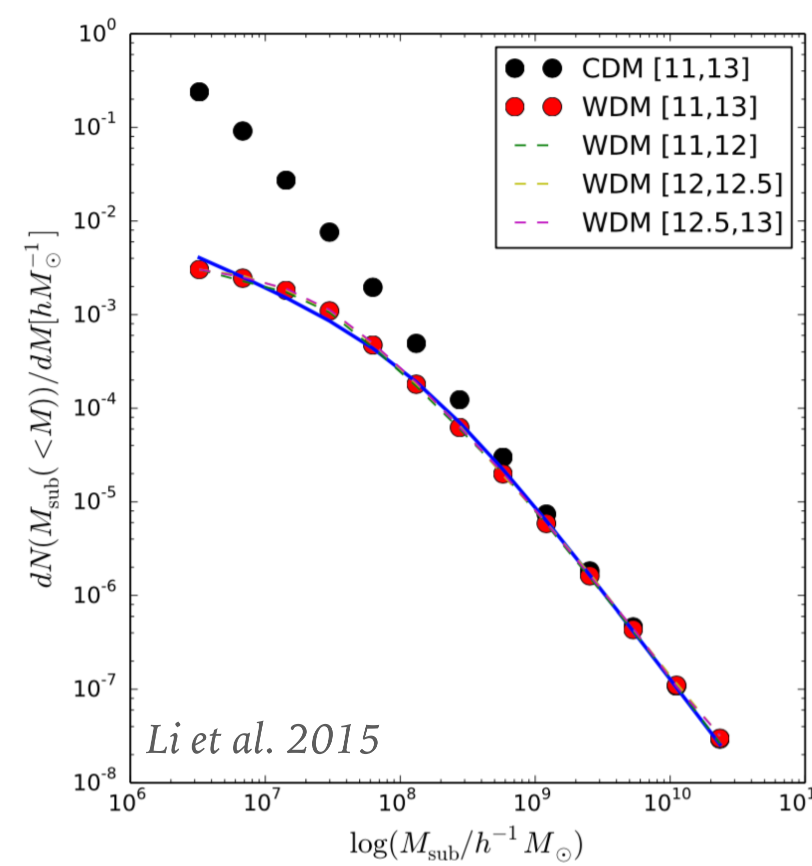

SIDM MODELS PROBED BY SL

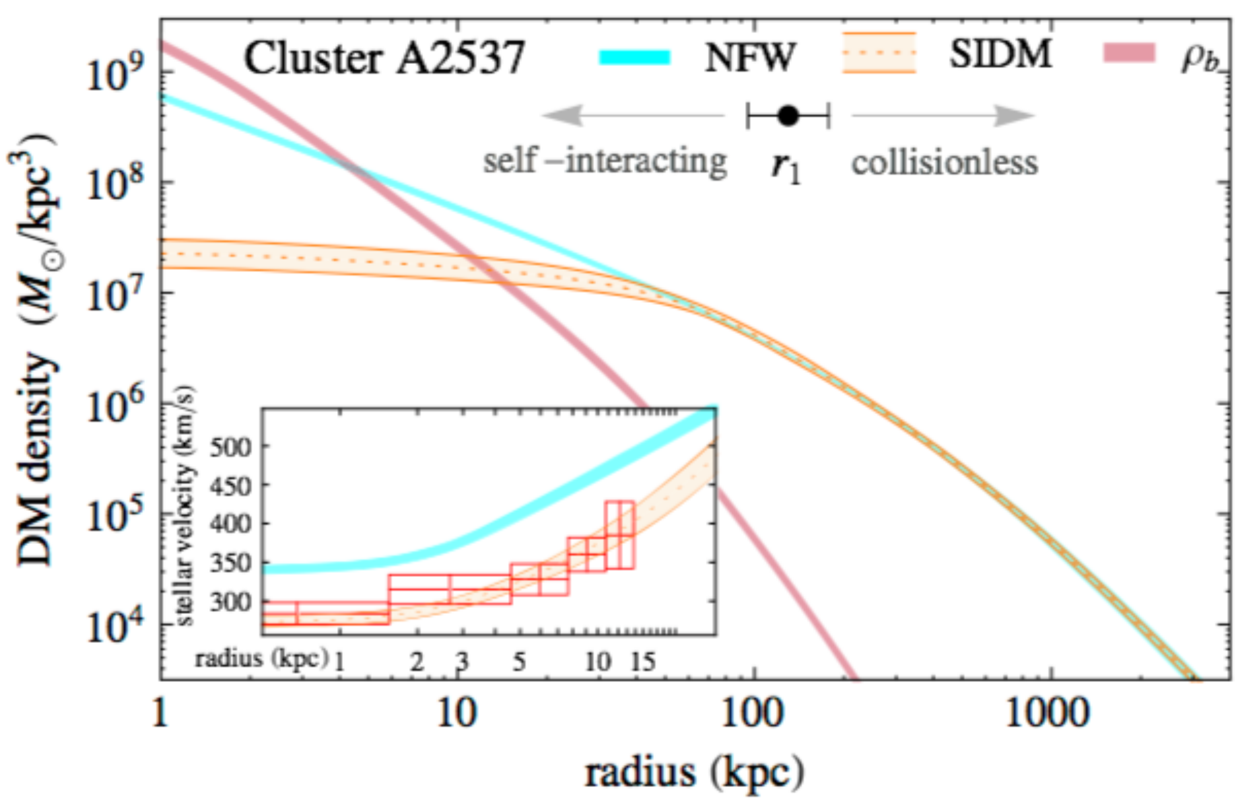

- Self-interaction cross sections between 0.1 and 2 cm^2/g may be consistent with observations of dwarf galaxies, LSBs and clusters
- the model of SIDM which is consistent with these data has a velocity dependent cross section
- interactions are more efficient in low velocity regimes, than in high velocity regimes

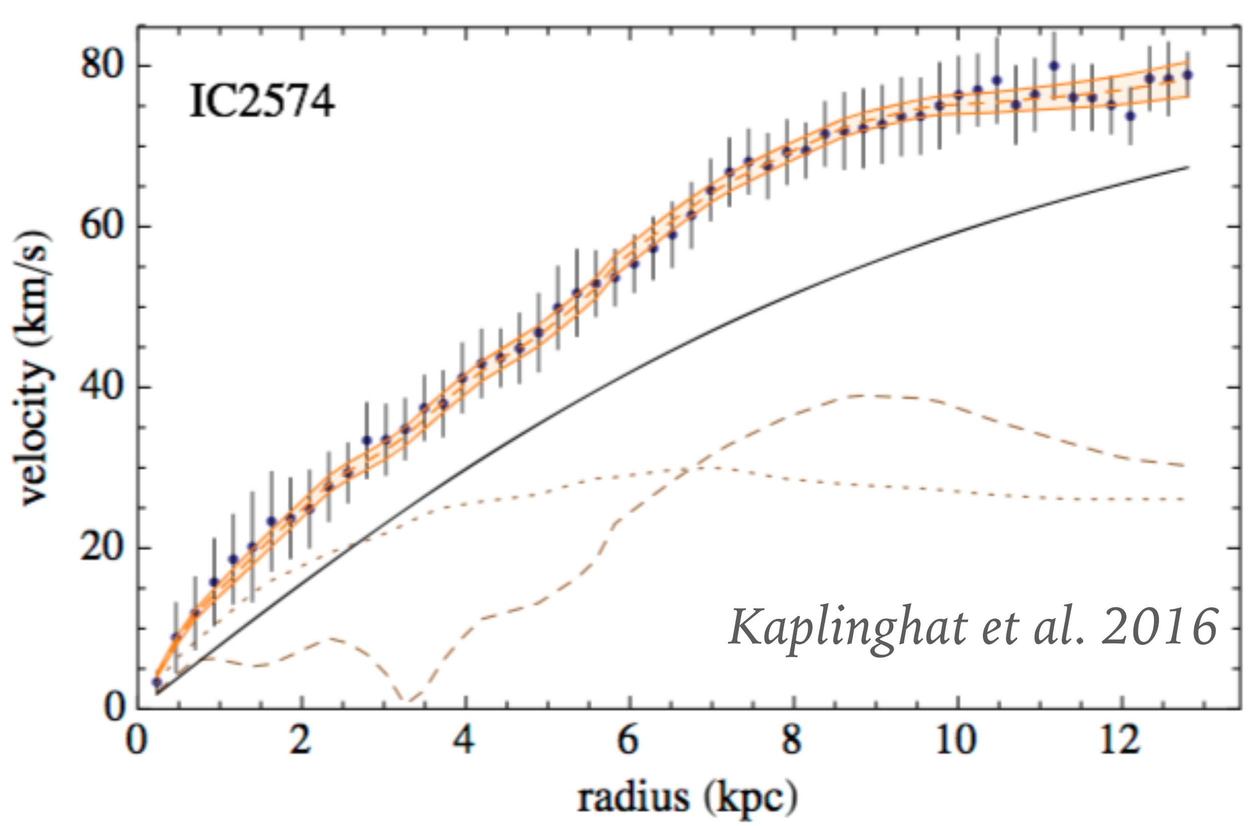

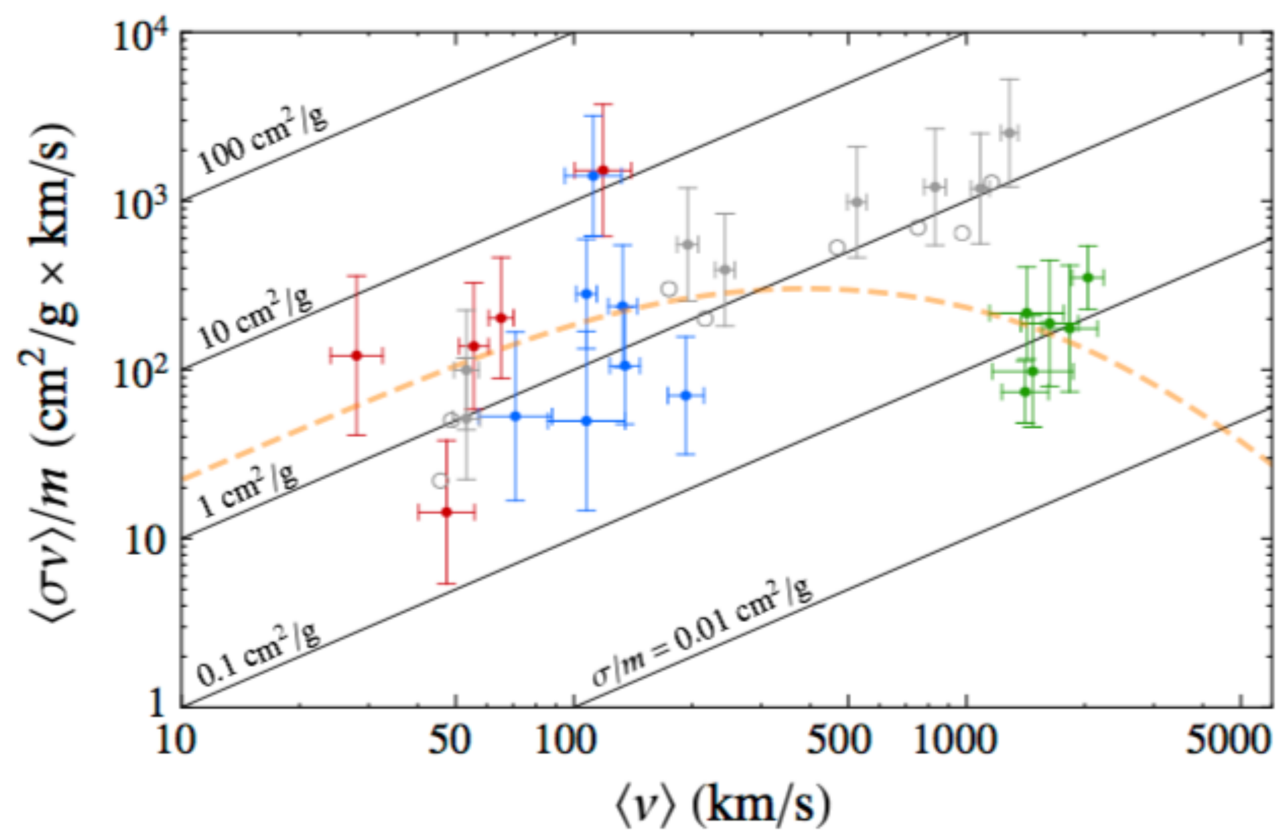

SIDM MODELS PROBED BY SL

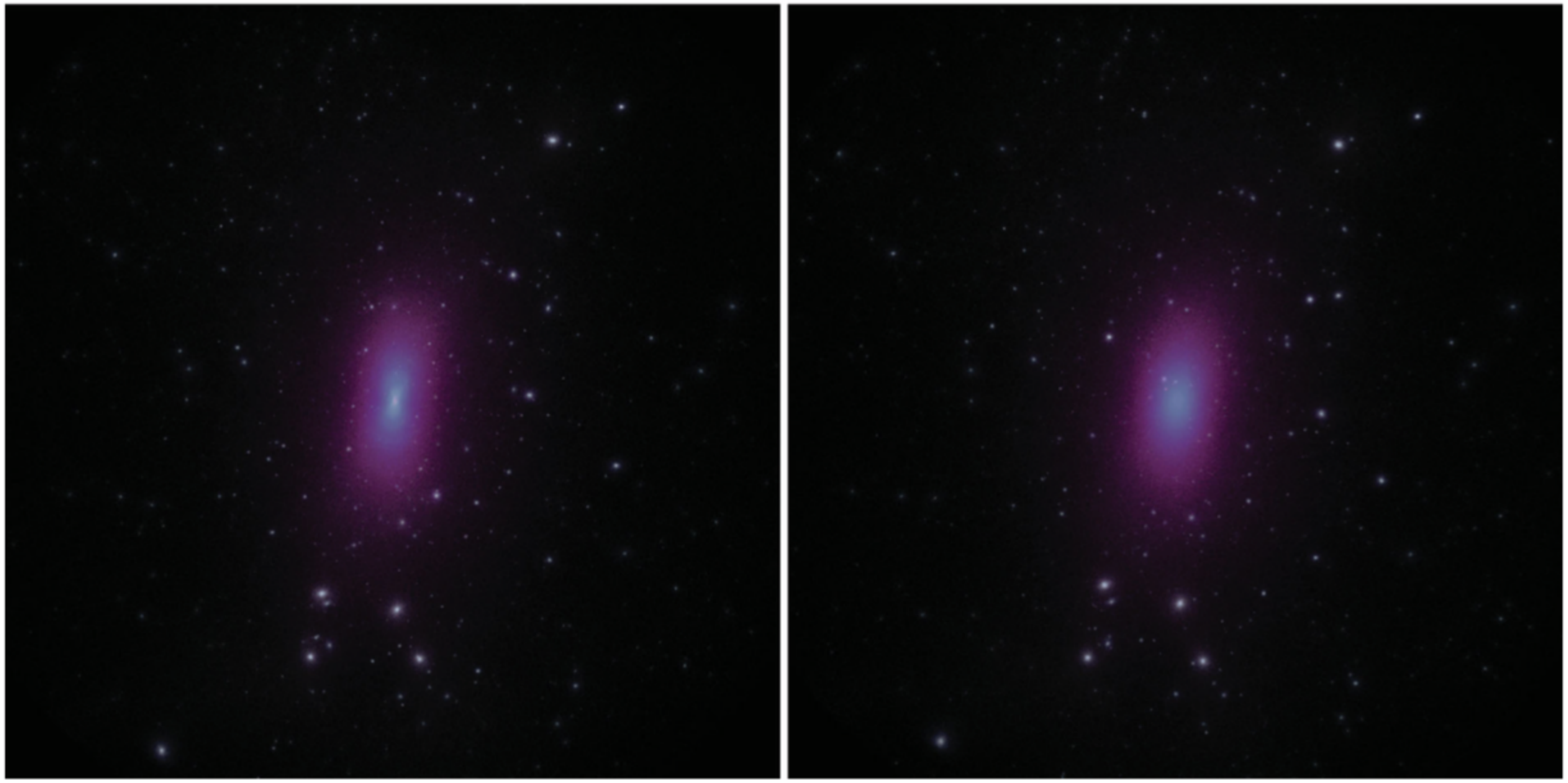

Rocha et al. 2013: numerical simulations of SIDM halos (but with velocity independent SI cross section)

Core circularization (see also Peter et al.2013)

Sub-halo "evaporation" (esp. in the core): trend with mass?

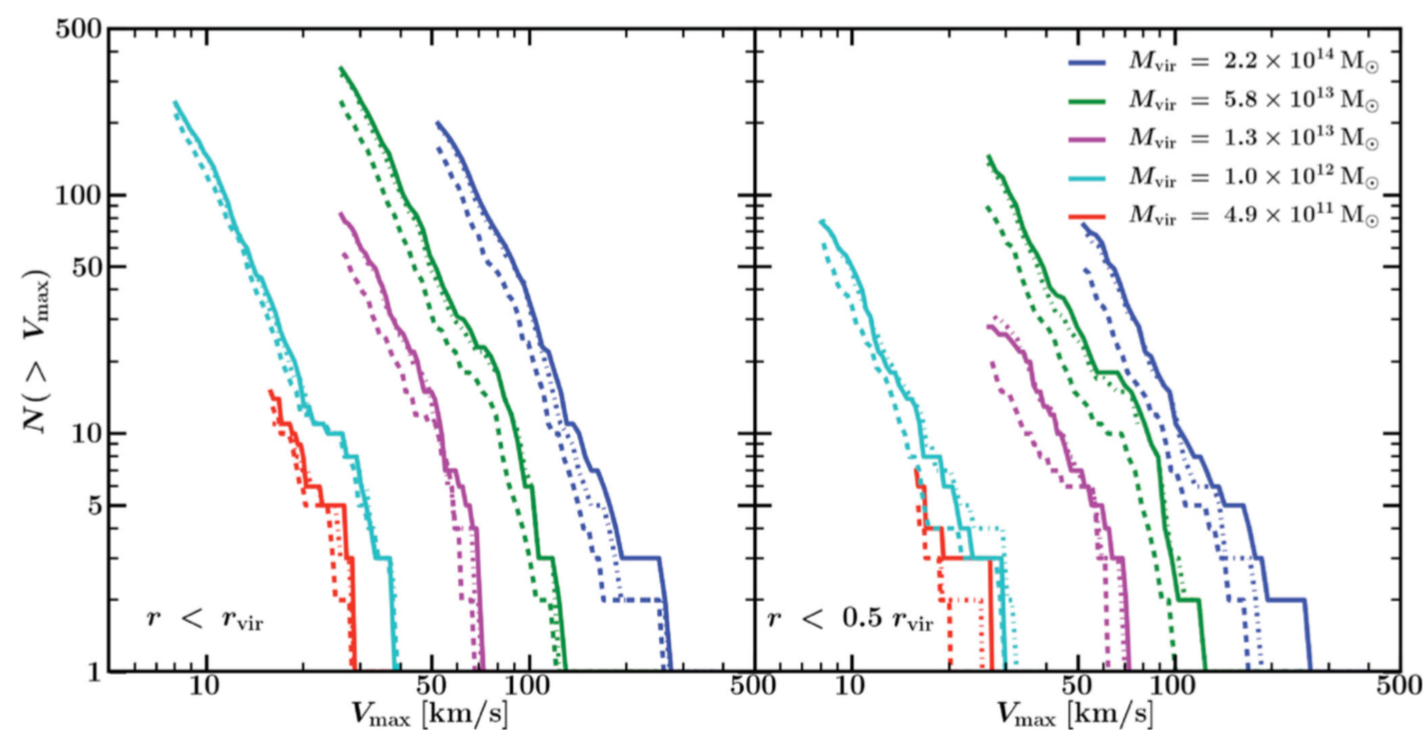

SUBHALOS/SUBSTRUCTURES AS A PROBE OF DM

- probing the mass function of DM sub-halos may be particularly useful to test scenarios such as WDM
- but also to test SIDM!
- Important thing to bear in mind: the typical scale of the ER in the case of a dwarf satellite is few mas (e.g. WDM)
- SL by galaxies in clusters may help to constrain the sub-halos on larger scales

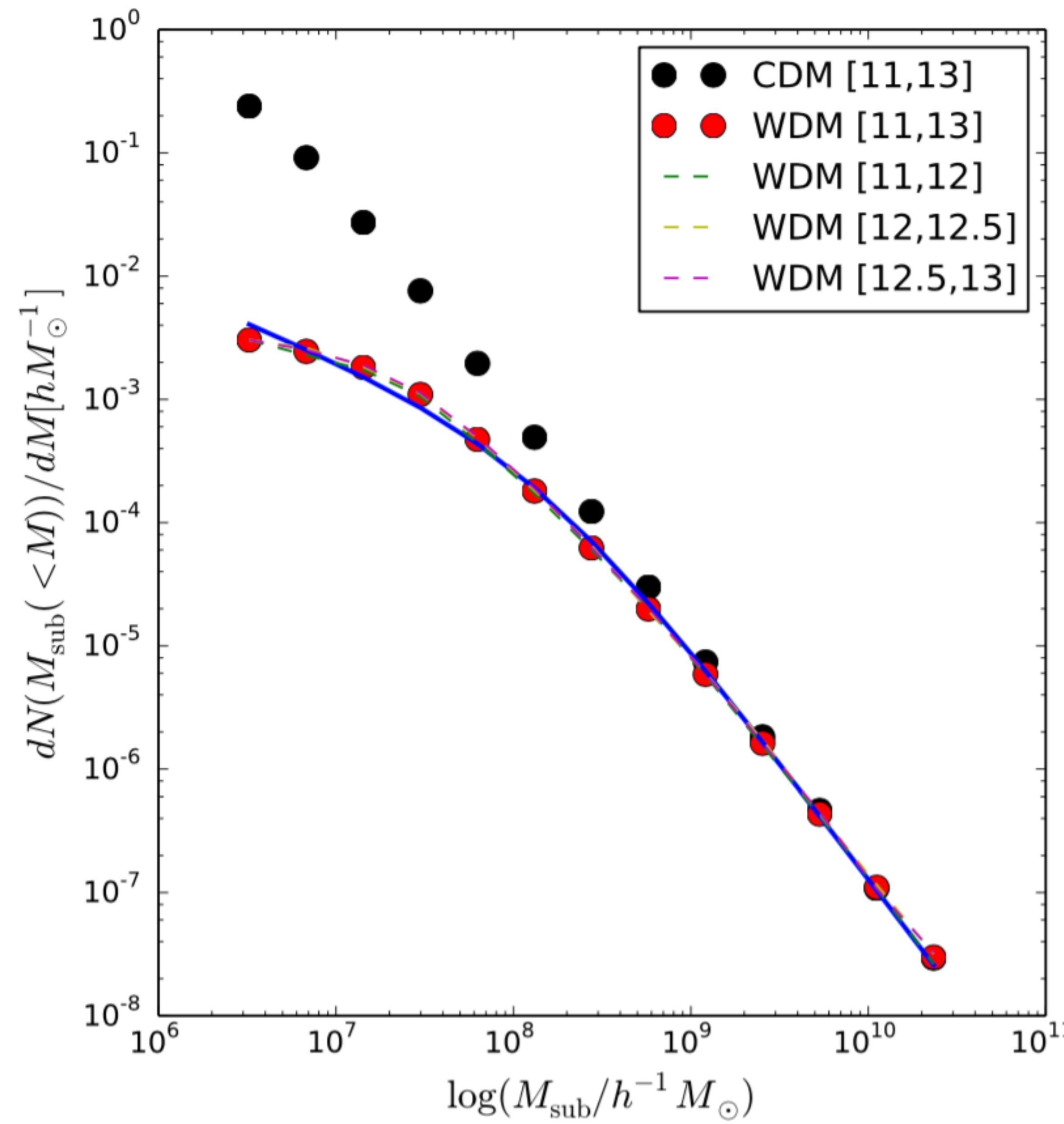

SUBSTRUCTURES FROM SL: FLUX ANOMALIES

- substructures detectable as magnification anomalies (second derivatives of the potential) of point like sources
  - easy to model
  - sensitive to wide range of masses
  - some theoretically established relations for cusp and fold images

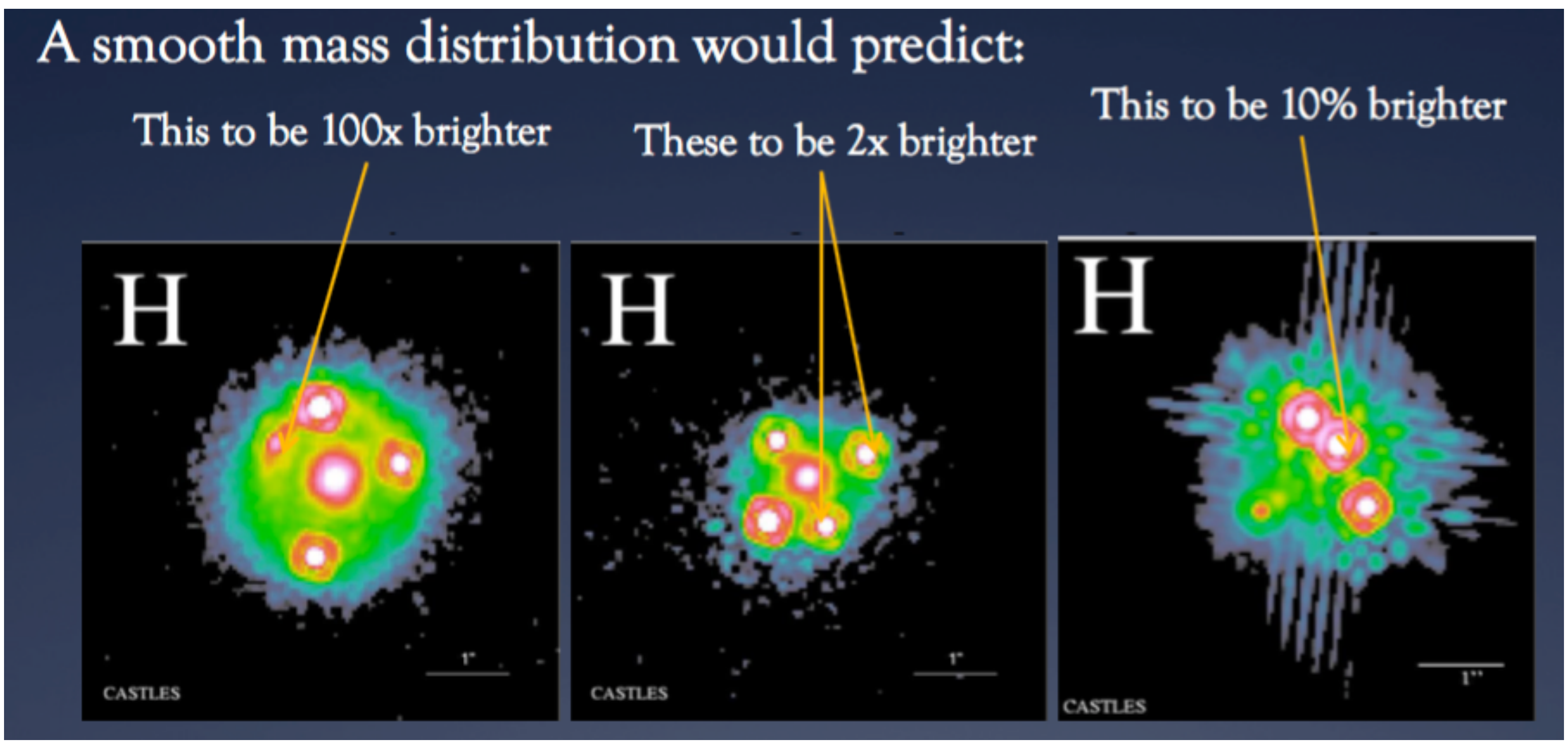

SUBSTRUCTURES FROM SL: FLUX ANOMALIES

detected in 7 radio lenses

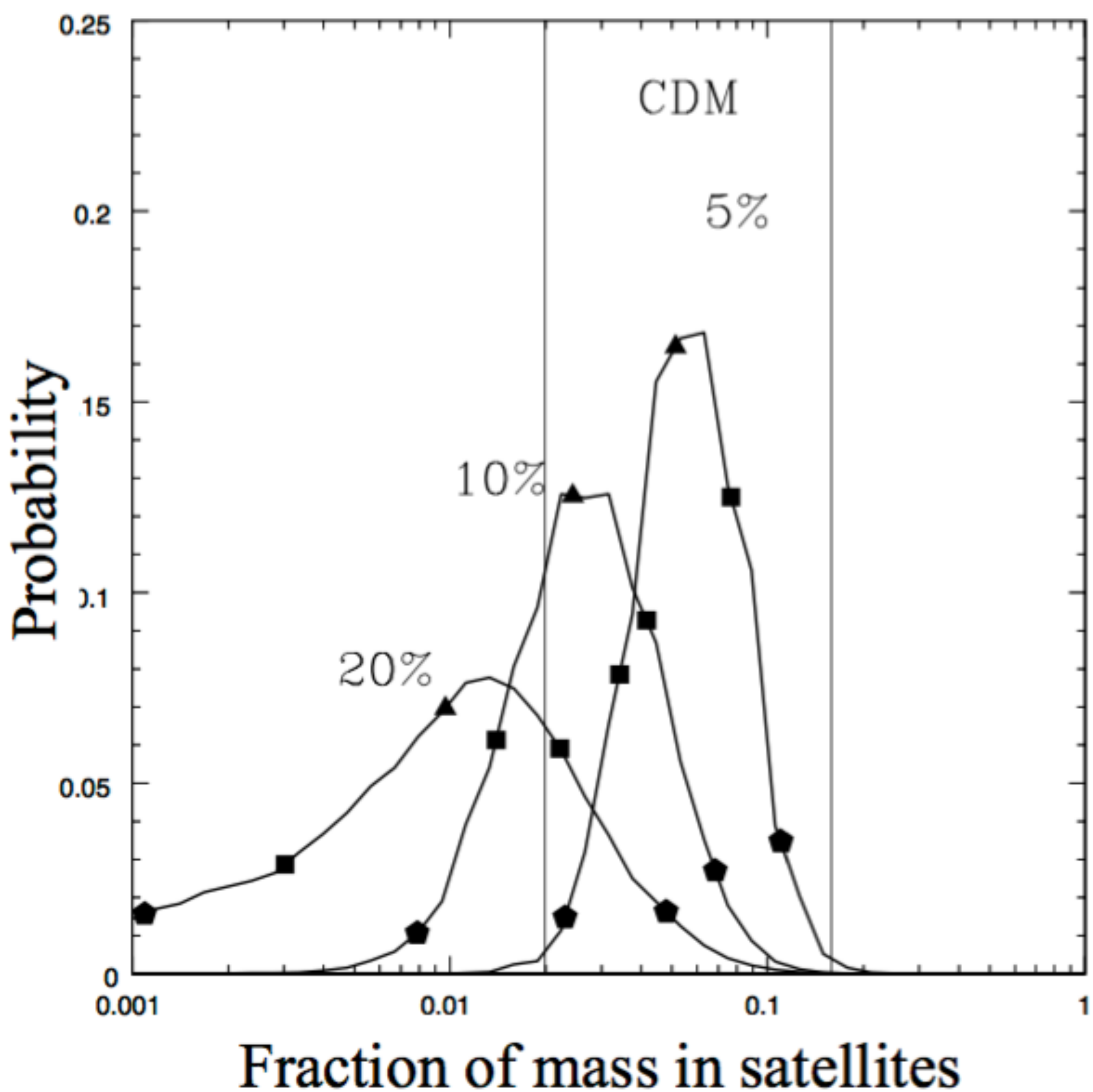

Dalal & Kochanek (2002): flux anomalies consistent with a fraction of mass in sub halos within the ER f~0.02

This is consistent with simulations in the framework of CDM

SUBSTRUCTURES FROM SL: GRAVITATIONAL IMAGING

- substructures are detected as surface brightness anomalies (i.e. astrometric anomalies, first derivatives of the potential)
  - sensitive to larger masses
  - becoming more efficient thanks to the achievement for higher resolutions: ALMA, adaptive optics, GVLBI (astrometric perturbations of the order of $\sim$10 mas)

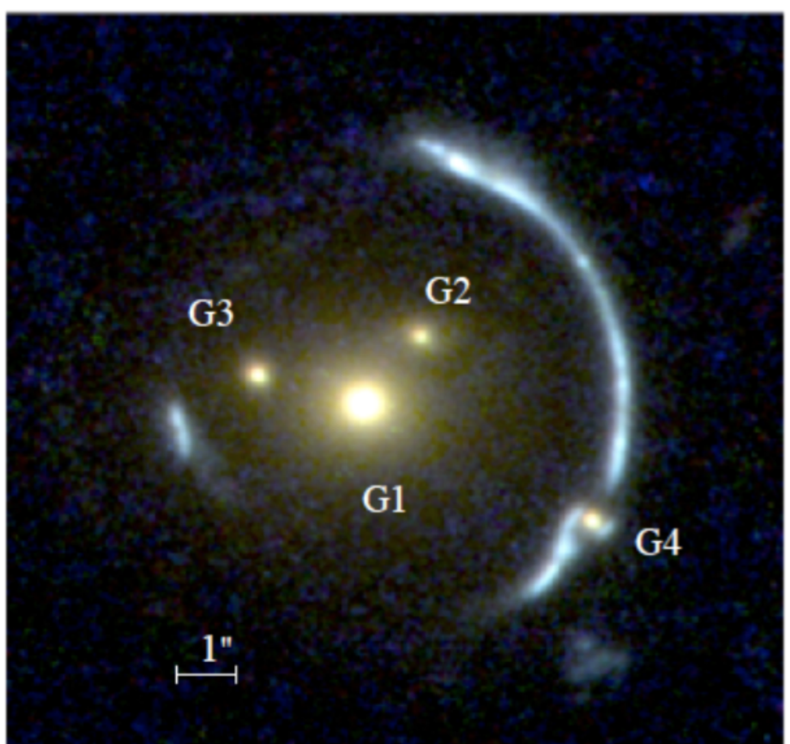

E.g. Vegetti et al. 2014

$$\psi(\mathbf{x},\eta)_{tot} = \psi(\mathbf{x},\eta) + \delta\psi(\mathbf{x})$$

$\psi(\mathbf{x},\eta)$ Smooth analytic power-law model

$\delta\psi(\mathbf{x})$ pixellated potential correction

SUBSTRUCTURES FROM SL: GRAVITATIONAL IMAGING

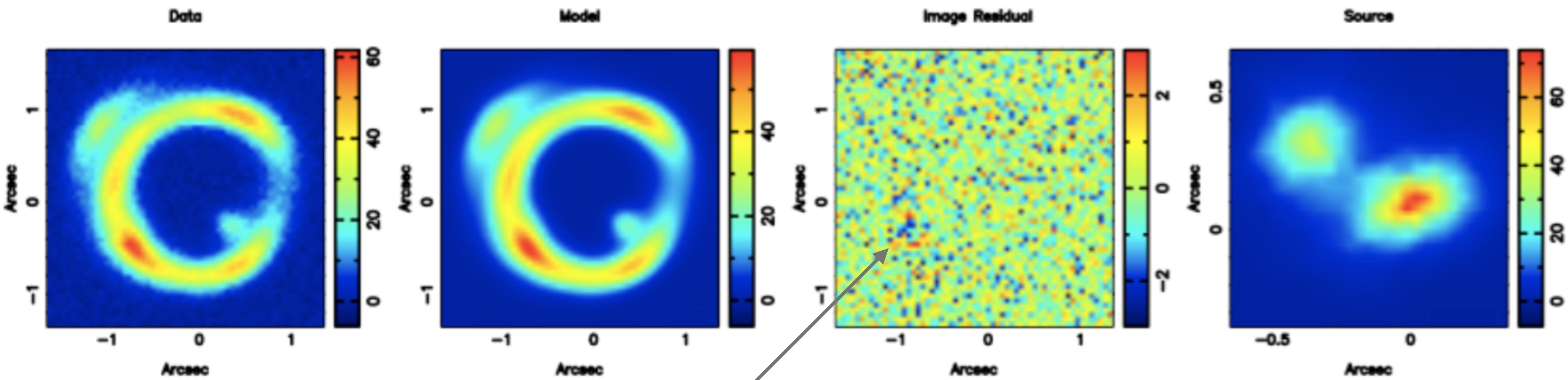

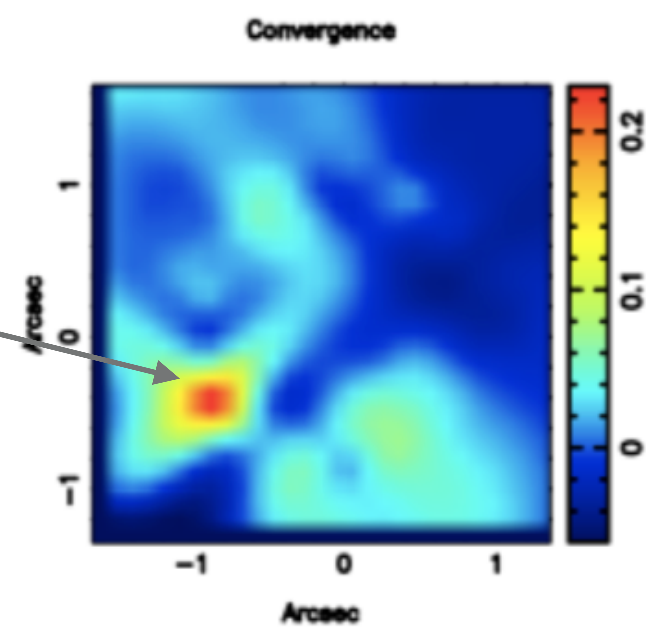

Substructures detected as corrections to a smooth potential

Density corrections

Issue: in addition to the usual modeling uncertainties, need to disentangle the structure in the potential from those in the sources

SUBSTRUCTURES FROM SL: GRAVITATIONAL IMAGING

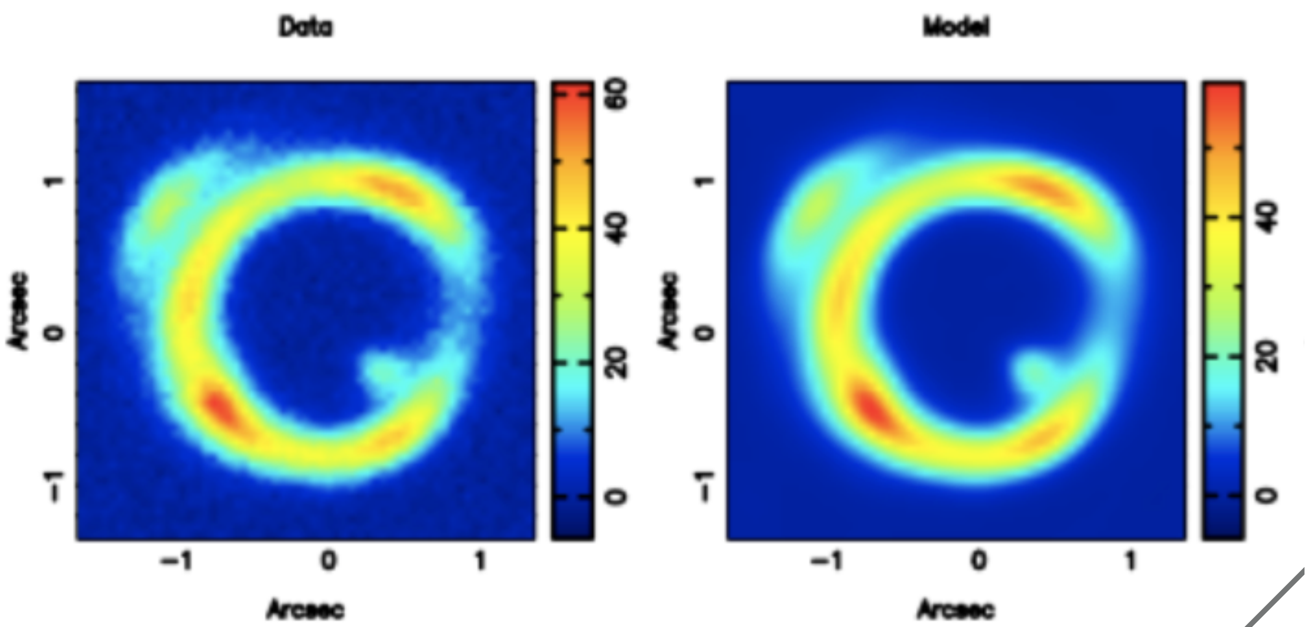

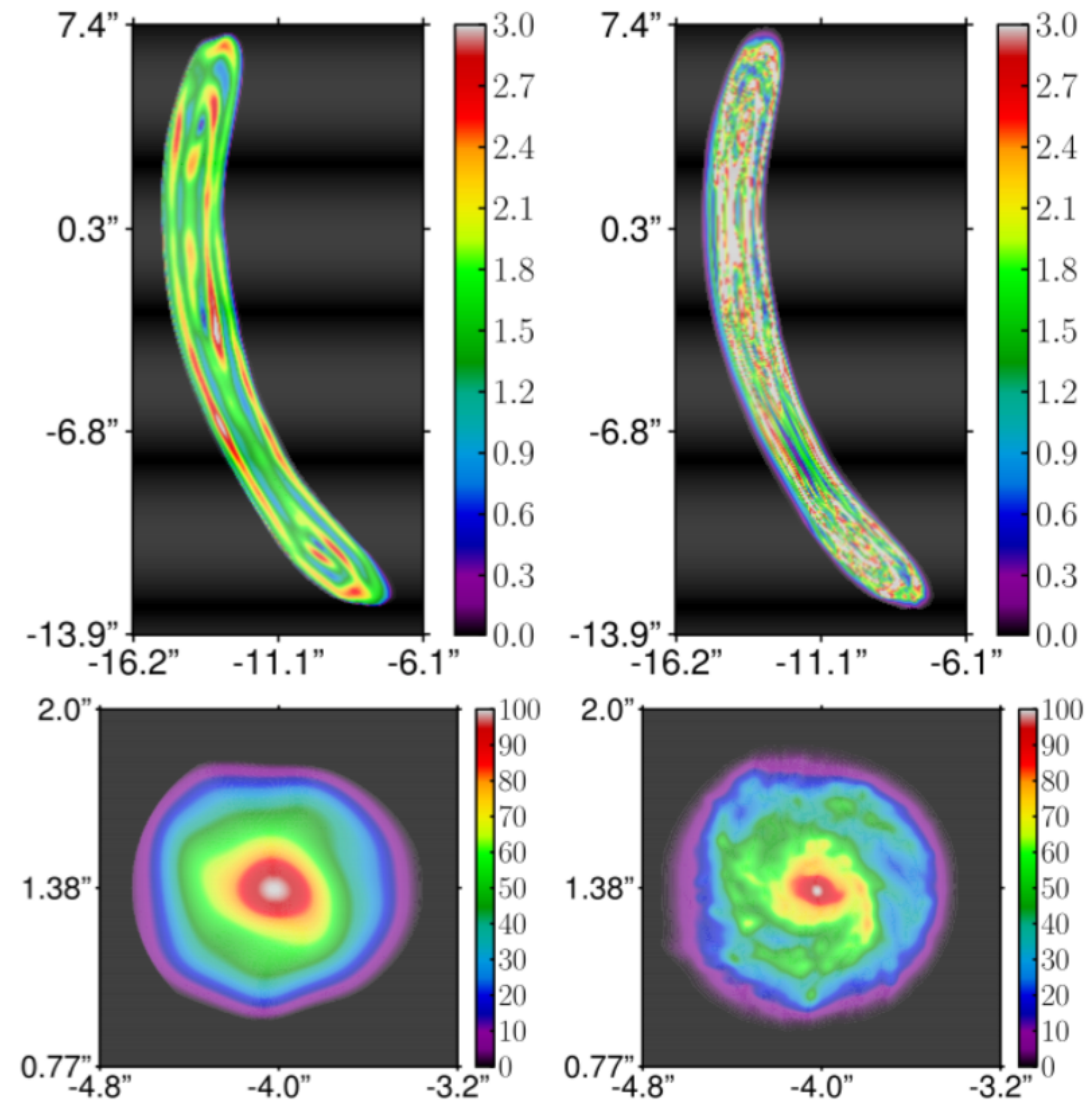

Substructures detected as corrections to a smooth potential

Issue: in addition to the usual modeling uncertainties, need to disentangle the structure in the potential from those in the sources

SUBSTRUCTURES FROM SL: GRAVITATIONAL IMAGING

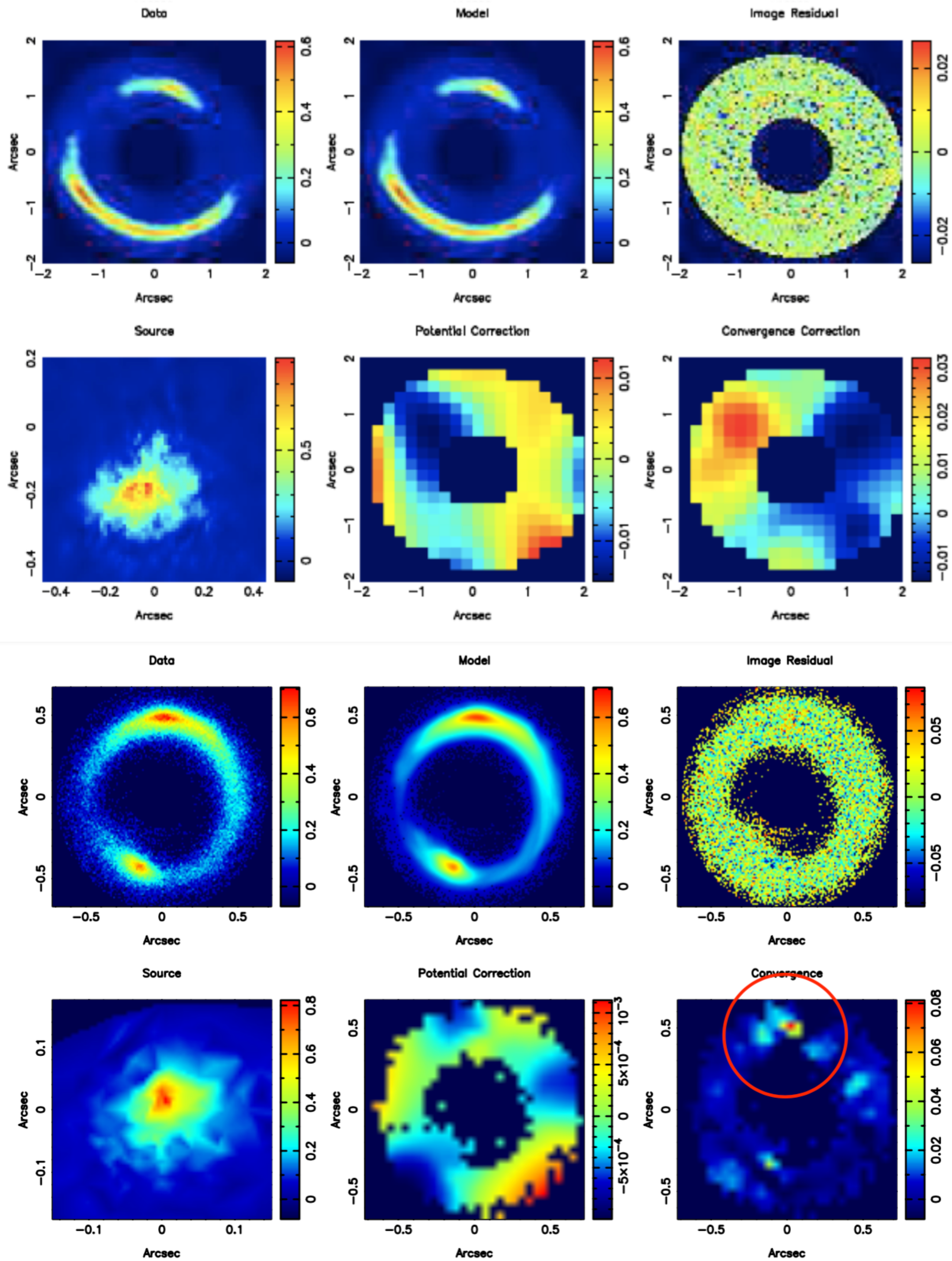

Vegetti et al. 2010, 2012, 2014:

substructures detected at high significance level (>10σ)

$$M_{\rm sub} \sim 2 - 40 \times 10^8 M_\odot$$

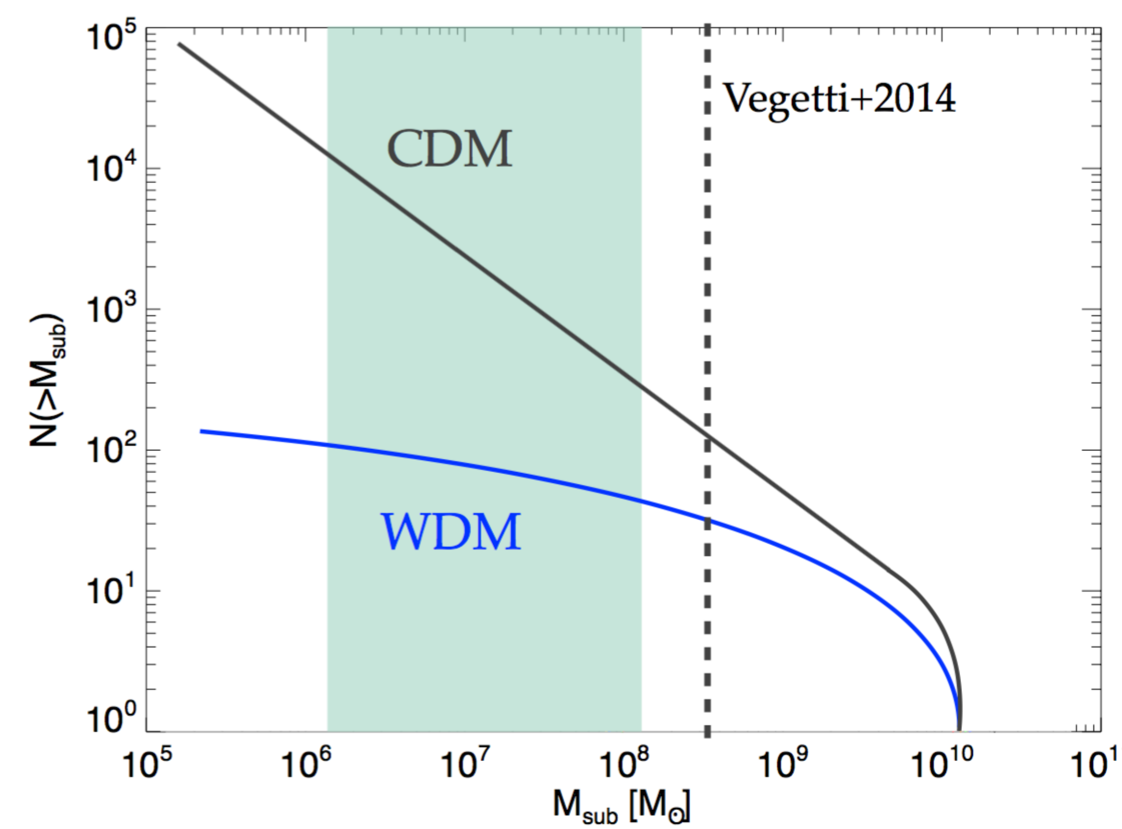

THE FRONTIER FIELDS INITIATIVE

(P.I. MATT MOUNTAIN, JENNIFER LOTZ)

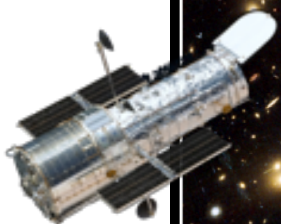

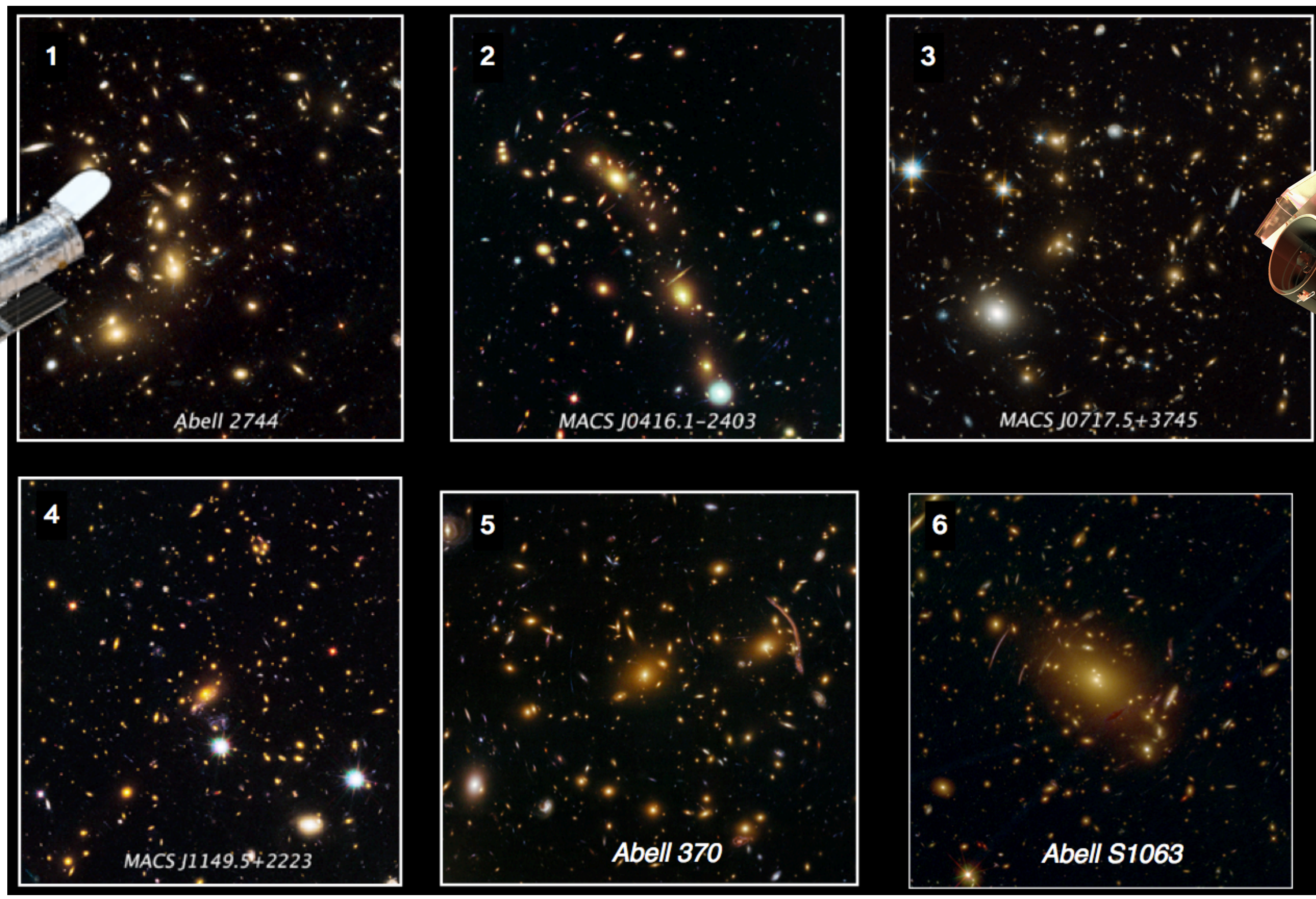

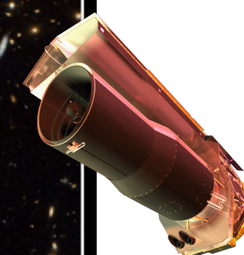

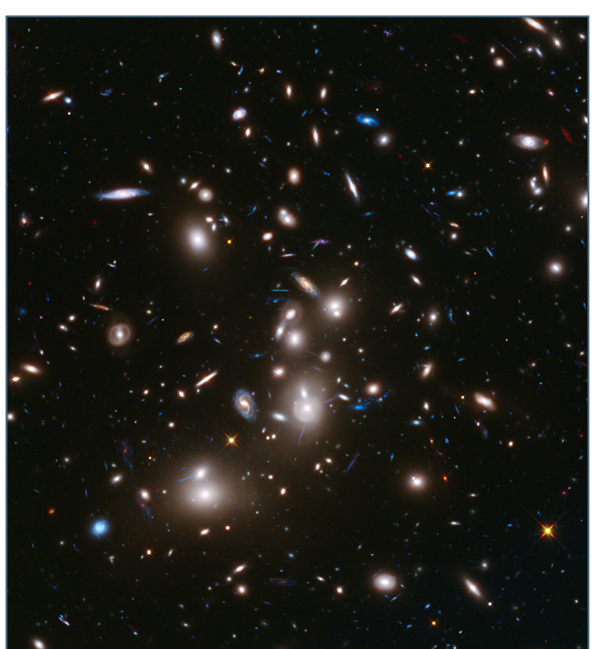

- 6 lensed + 6 parallel fields
- 840 Hubble orbits +1000 Spitzer hrs directors' discretionary time
- Cycles 21, 22, 23
- Strongest lenses with low zodiacal bkg, galactic extinction, observable with ALMA
- Complemented by Chandra, Subaru, VLT Hawk-I, Gemini, spectra from Keck, Photo-z

ACS: (70 orbits per position)			WFC3/IR: (70 orbits per position)		
Filter	Orbits	AB_mag	Filter	Orbits	AB_mag
F435W	18	28.8	F105W	24	28.9
F606W	10	28.8	F125W	12	28.6
F814W	42	29.1	F140W	10	28.6
			F160W	24	28.7

Cluster Name	z	Cluster		Parallel Field		HST FOV	Regions File
		RA	Dec	RA	Dec		
Year 1:							
Abell 2744	0.308	00:14:21.2	-30:23:50.1	00:13:53.6	-30:22:54.3		regions
MACSJ0416.1-2403	0.396	04:16:08.9	-24:04:28.7	04:16:33.1	-24:06:48.7		regions
Year 2:							
MACSJ0717.5+3745	0.545	07:17:34.0	+37:44:49.0	07:17:17.0	+37:49:47.3		regions
MACSJ1149.5+2223	0.543	11:49:36.3	+22:23:58.1	11:49:40.5	+22:18:02.3		regions
Year 3:							
Abell S1063 (RXCJ2248.7-4431)	0.348	22:48:44.4	-44:31:48.5	22:49:17.7	-44:32:43.8		regions
Abell 370	0.375	02:39:52.9	-01:34:36.5	02:40:13.4	-01:37:32.8		regions

Frontier Fields Visit Status Page

[How To Use This Page]

Observed Scheduling Long Range Planning High Level Science Products (full-depth mosaics)

	Progress	2013 Oct	2013 Nov	2013 Dec	2014 Jan	2014 Feb	2014 Mar	2014 Apr	2014 May	2014 Jun	2014 Jul	2014 Aug	2014 Sep	2014 Oct	2014 Nov	2014 Dec
ABELL-2744	100.0%	WFC3	WFC3						ACS	ACS	ACS					
ABELL-2744-HFFPAR	100.0%	ACS	ACS						WFC3	WFC3	WFC3					
MACSJ0416.1-2403	100.0%				ACS	ACS					WFC3	WFC3	WFC3			
MACSJ0416.1-2403-HFFPAR	100.0%				WFC3	WFC3					ACS	ACS	ACS			
MACSJ0717.5+3745	50.0%	ACS											ACS	ACS	ACS	
MACSJ0717.5+3745-HFFPAR	50.0%	WFC3											WFC3	WFC3	WFC3	
MACSJ1149.5+2223	51.4%		WFC3					ACS							WFC3	WFC3
MACSJ1149.5+2223-HFFPAR	51.4%		ACS					WFC3							ACS	ACS
ABELL-S1063	1.4%													ACS		
ABELL-S1063-HFFPAR	1.4%													WFC3		

	2015 Jan	2015 Feb	2015 Mar	2015 Apr	2015 May	2015 Jun	2015 Jul	2015 Aug	2015 Sep	2015 Oct	2015 Nov	2015 Dec	2016 Jan	2016 Feb	2016 Mar	2016 Apr	2016 May	2016 Jun	2016 Jul
ABELL-2744																			
ABELL-2744-HFFPAR																			
MACSJ0416.1-2403																			
MACSJ0416.1-2403-HFFPAR																			
MACSJ0717.5+3745		WFC3	WFC3	WFC3															
MACSJ0717.5+3745-HFFPAR		ACS	ACS	ACS															
MACSJ1149.5+2223	WFC3			ACS	ACS	ACS													
MACSJ1149.5+2223-HFFPAR	ACS			WFC3	WFC3	WFC3													
ABELL-S1063									ACS	ACS	ACS	ACS				WFC3	WFC3	WFC3	WFC3
ABELL-S1063-HFFPAR									WFC3	WFC3	WFC3	WFC3				ACS	ACS	ACS	ACS

[HST Frontier Fields Data Overview]
[HST Frontier Fields Archive Data Products Page]

MAST High Level Data Pages:

- ABELL-2744 + Parallel Field
- MACSJ0416.1-2403 + Parallel Field
- MACSJ0717.5+3745 + Parallel Field
- MACSJ1149.5+2223 + Parallel Field
- ABELL-S1063 + Parallel Field

Last updated: 2015-02-04T19:01:21.163230

MACSJ0416 **1. Before HFF …**

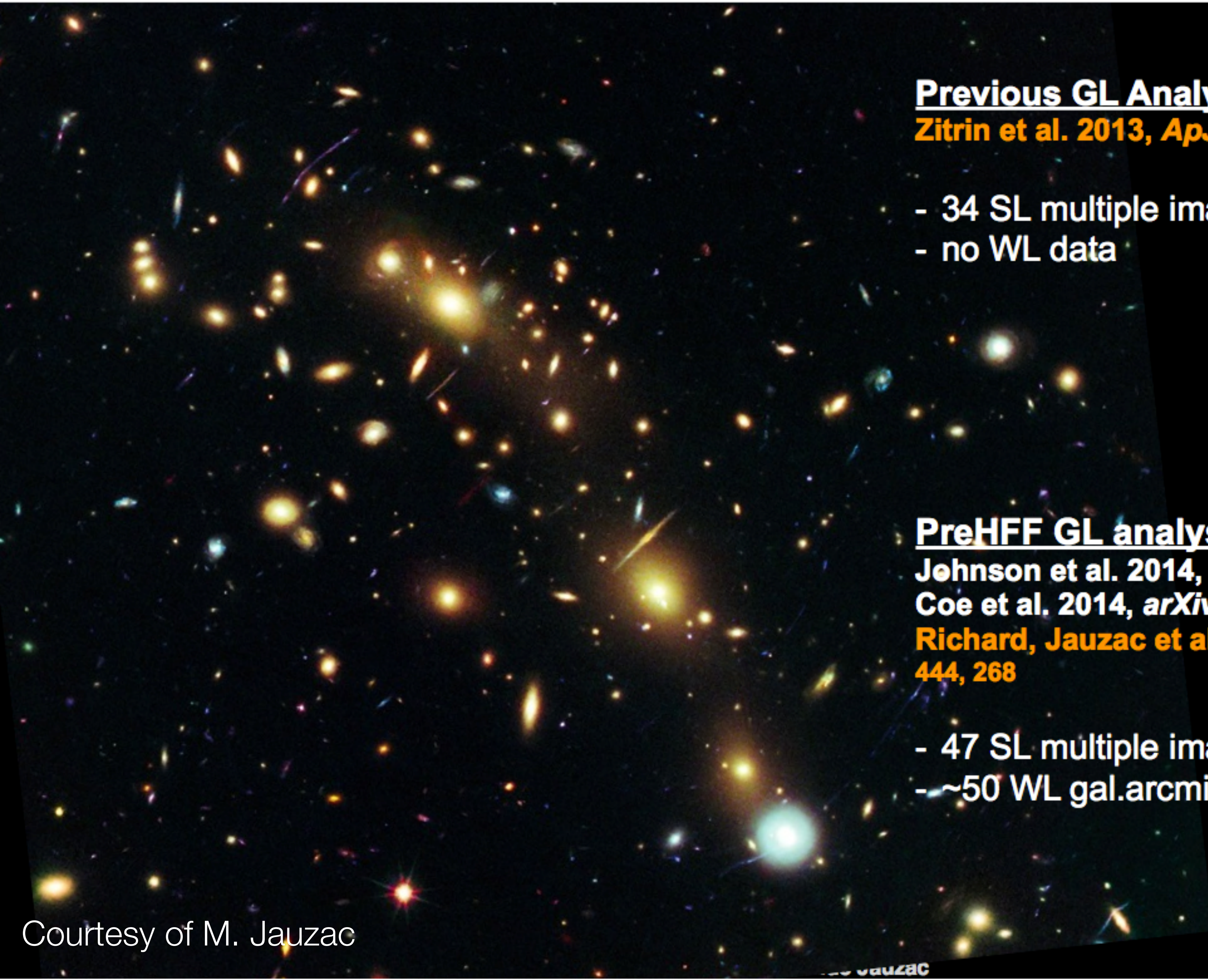

Previous GL Analysis :
Zitrin et al. 2013, *ApJ, 762, 30*

- 34 SL multiple images
- no WL data

PreHFF GL analysis :
Johnson et al. 2014, *arXiv 1405.0222*
Coe et al. 2014, *arXiv 1405.0011*
Richard, Jauzac et al. 2014, MNRAS, 444, 268

- 47 SL multiple images
- ~50 WL gal.arcmin^{-2}

Courtesy of M. Jauzac

1. ... After HFF !!!

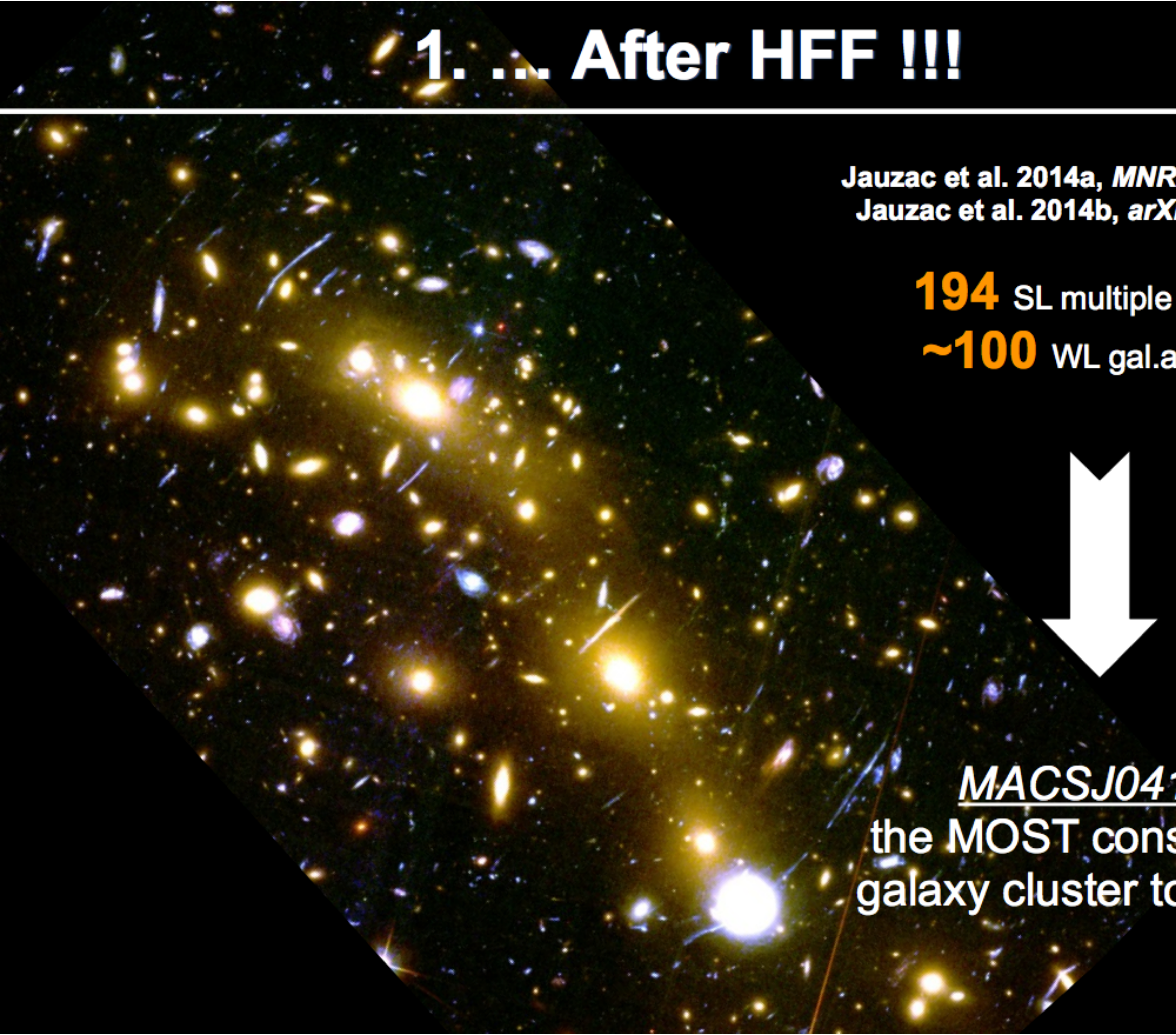

Jauzac et al. 2014a, *MNRAS, 443, 1549*
Jauzac et al. 2014b, *arXiv, 1406.3011*

194 SL multiple images
~100 WL gal.arcmin^{-2}

MACSJ0416 :
the MOST constrained
galaxy cluster to date !!!

STRONG GALAXY-GALAXY LENSING IN CLUSTERS

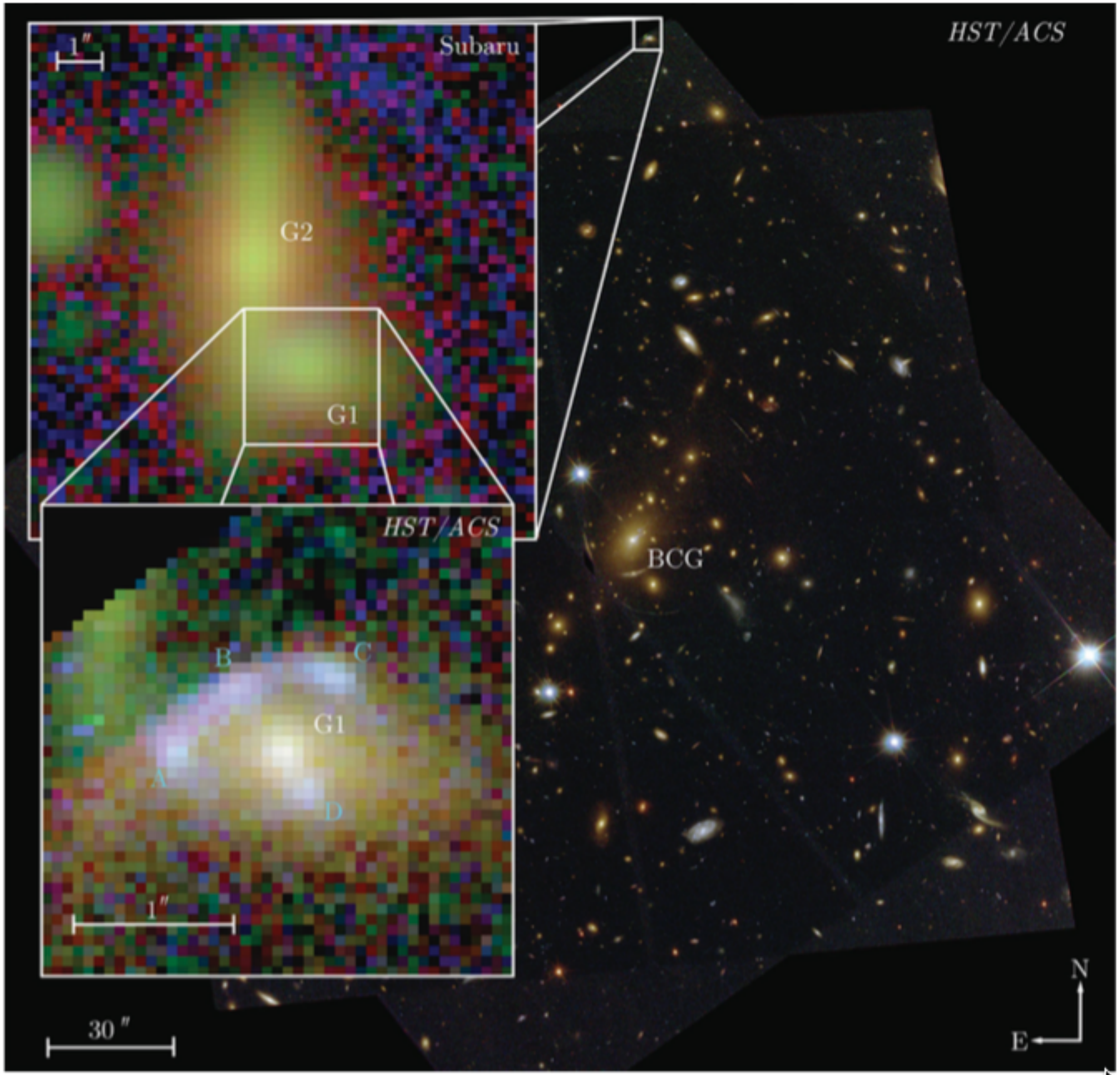

Parry et al. 2016

FRONTIER FIELDS: AN EXCESS OF DM SUB HALOS COMPARED TO SIMULATIONS?

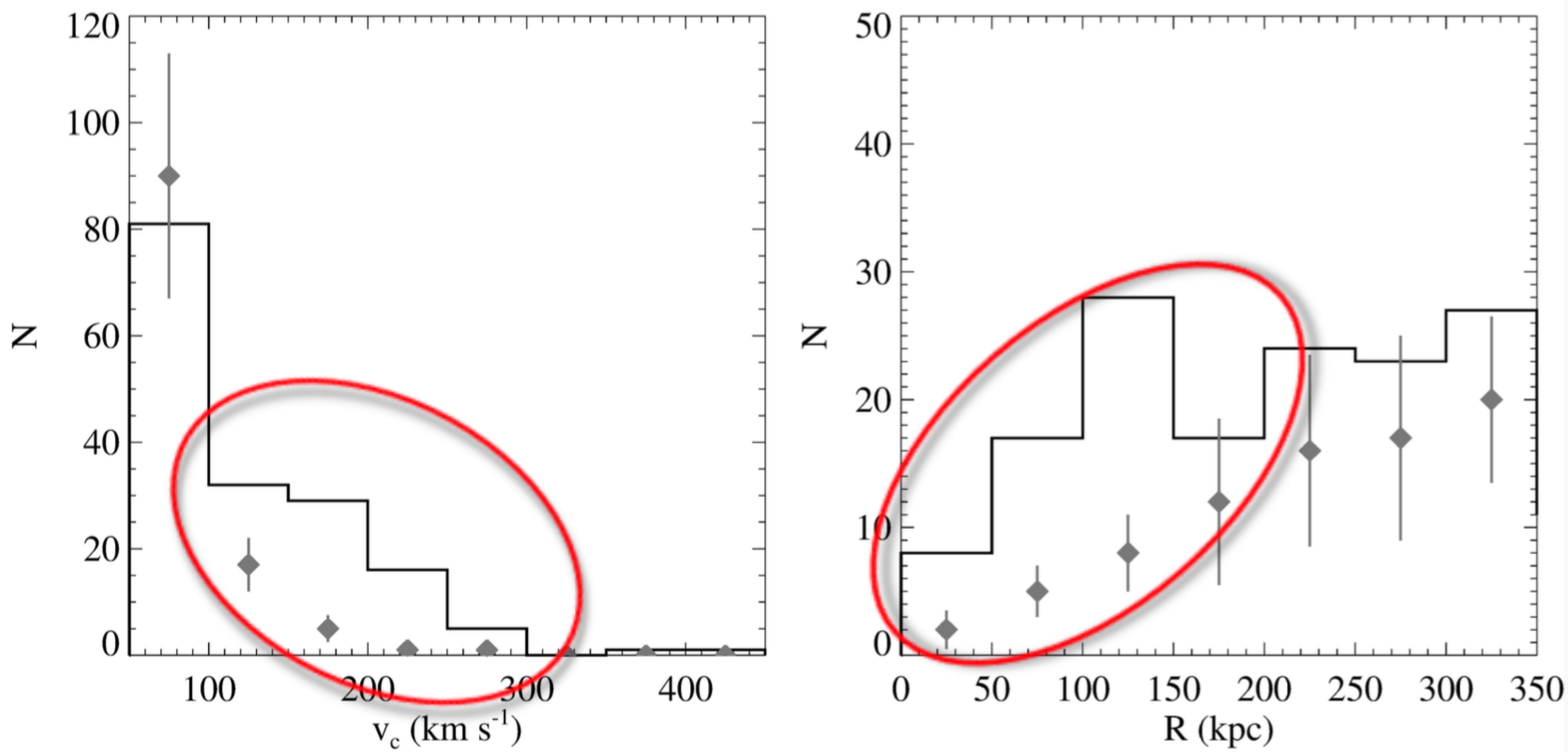

MACS J0416 - Grillo+15a

COSMOGRAPHY WITH TIME DELAYS

Treu & Marshall, 2016

Time delay distance $\propto \dfrac{1}{H_0}$

Distances encode information on additional cosmological parameters!

$$\tau(\boldsymbol{\theta}) = \frac{D_{\Delta t}}{c} \cdot \Phi(\boldsymbol{\theta}, \boldsymbol{\beta}),$$

$$\text{where } \Phi(\boldsymbol{\theta}) = \frac{1}{2}(\boldsymbol{\theta} - \boldsymbol{\beta})^2 - \psi(\boldsymbol{\theta}).$$

Obtain from the lens mass model

- Needed ingredients:
  - Time delays
  - lens mass model

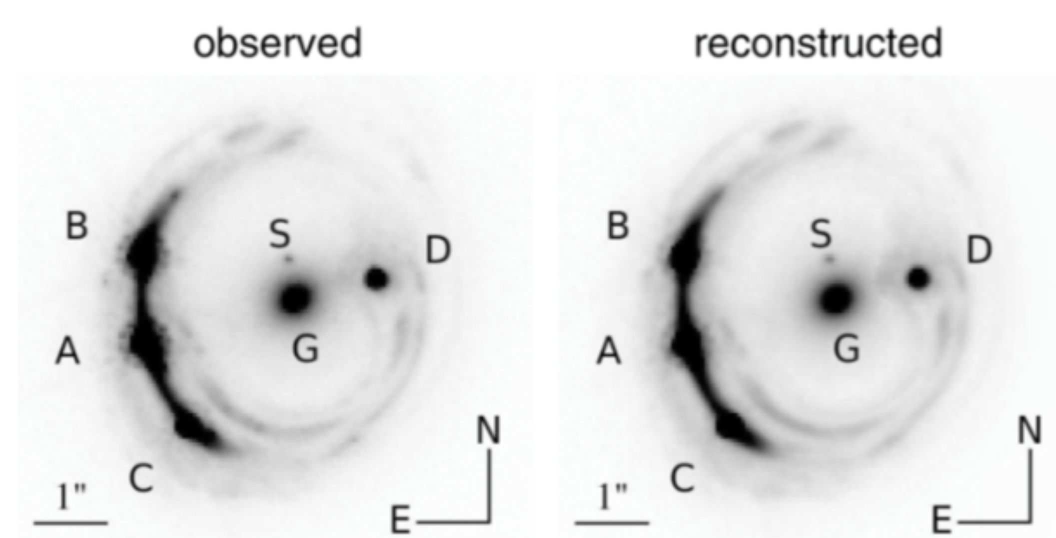

THE HUBBLE CONSTANT FROM TIME DELAYS

ON THE POSSIBILITY OF DETERMINING HUBBLE'S PARAMETER AND THE MASSES OF GALAXIES FROM THE GRAVITATIONAL LENS EFFECT*

Sjur Refsdal

(Communicated by H. Bondi)

(Received 1964 January 27)

Summary

The gravitational lens effect is applied to a supernova lying far behind and close to the line of sight through a distant galaxy. The light from the supernova may follow two different paths to the observer, and the difference Δt in the time of light travel for these two paths can amount to a couple of months or more, and may be measurable. It is shown that Hubble's parameter and the mass of the galaxy can be expressed by Δt, the red-shifts of the supernova and the galaxy, the luminosities of the supernova " images " and the angle between them. The possibility of observing the phenomenon is discussed.

1. *Introduction*.—In 1937 Zwicky suggested that a galaxy, due to the gravitational deflection of light, may act as a gravitational lens. He considered the case of a galaxy A lying far behind and close to the line of sight through a distant galaxy B. If the line of sight through the centre of B goes through A, the "image" of A will be a ring around B, otherwise two separated "images" appear, on opposite sides of B. The phenomenon has later been discussed by Zwicky (1957) and Klimov (1963), and they both conclude that the possibility of observing the phenomenon should be good. In the present paper the case of a supernova

TABLE 2

HUBBLE CONSTANT FROM EACH LENS SYSTEM

Lens Name	h (1 σ Range)
B0218+357	0.21 (. . .)
HE 0435−1223	1.02 (0.70–1.39)
RX J0911+0551	0.96 (0.75–1.21)
SBS 0909+532	0.84 (0.47–)
FBQ 0951+2635	0.67 (0.56–0.81)
Q0957+561	0.99 (0.82–1.17)
HE 1104−1805	1.04 (0.92–1.22)
PG 1115+080	0.66 (0.49–0.84)
RX J1131−1231	0.79 (0.59–1.03)
B1422+231	0.16 (–0.36)
SBS 1520+530	0.53 (0.46–0.61)
B1600+434	0.65 (0.54–0.77)
B1608+656	0.89 (0.77–1.20)
SDSS J1650+4251	0.53 (0.44–0.63)
PKS 1830−211	0.88 (0.58–)
HE 2149−2745	0.69 (0.57–0.82)
All	0.70 (0.68–0.73)

NOTE.—The Hubble constant and its error are estimated from the effective χ^2.

Oguri et al. 2007

CURRENT MEASUREMENTS OF TIME DELAYS

Enormous progress in the quality of the light curves since the first measurements thanks to dedicated networks of telescopes. For example: the COSMOGRAIL project measured time delays with precision <4% for 5 lenses

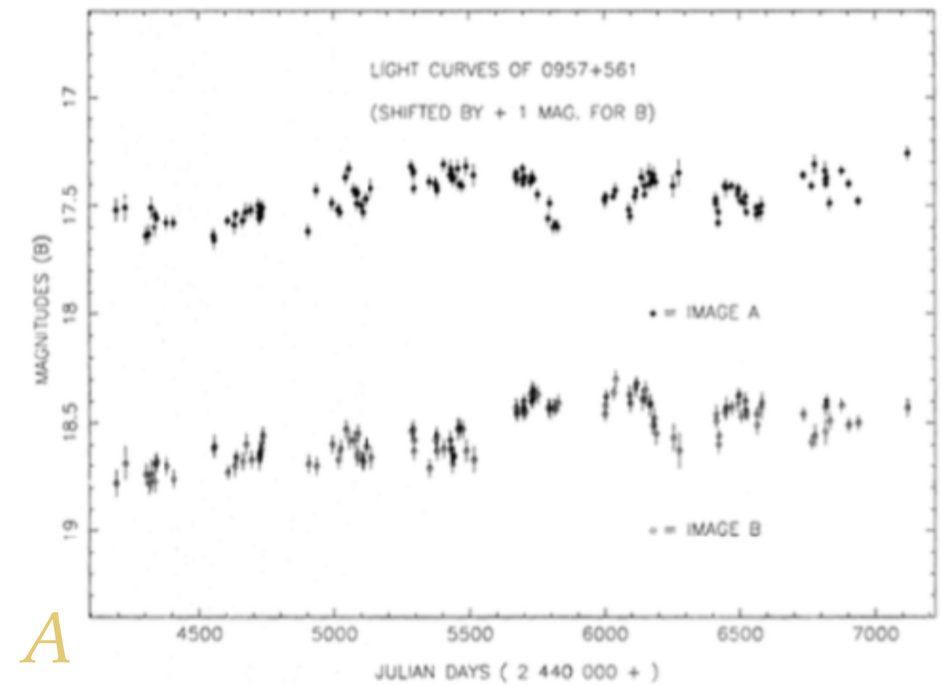

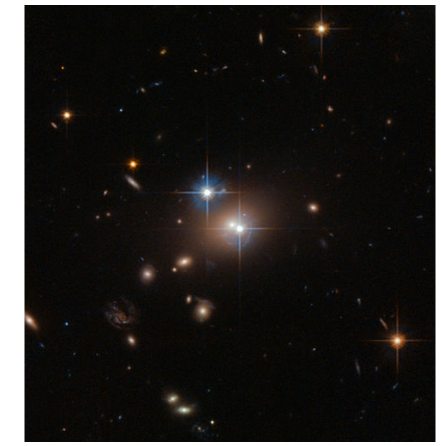

0957+561

Vanderriest et al. 1989

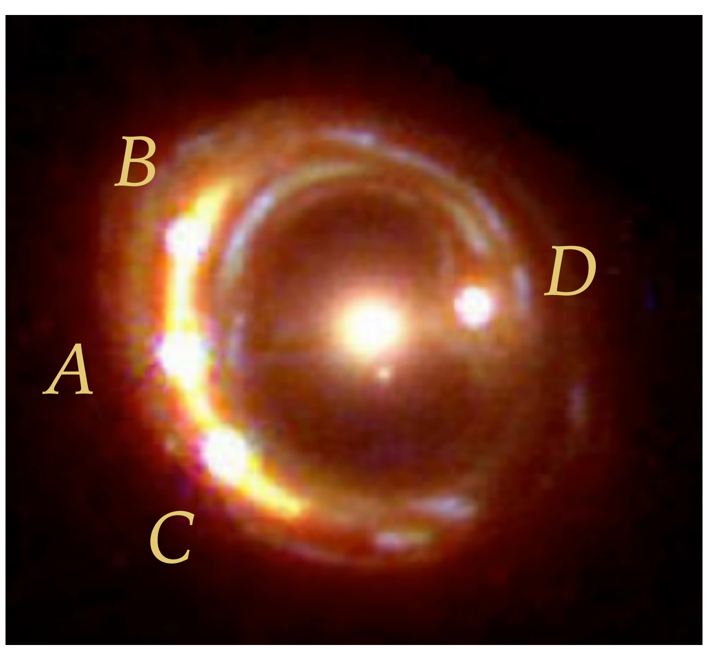

RXJ1131

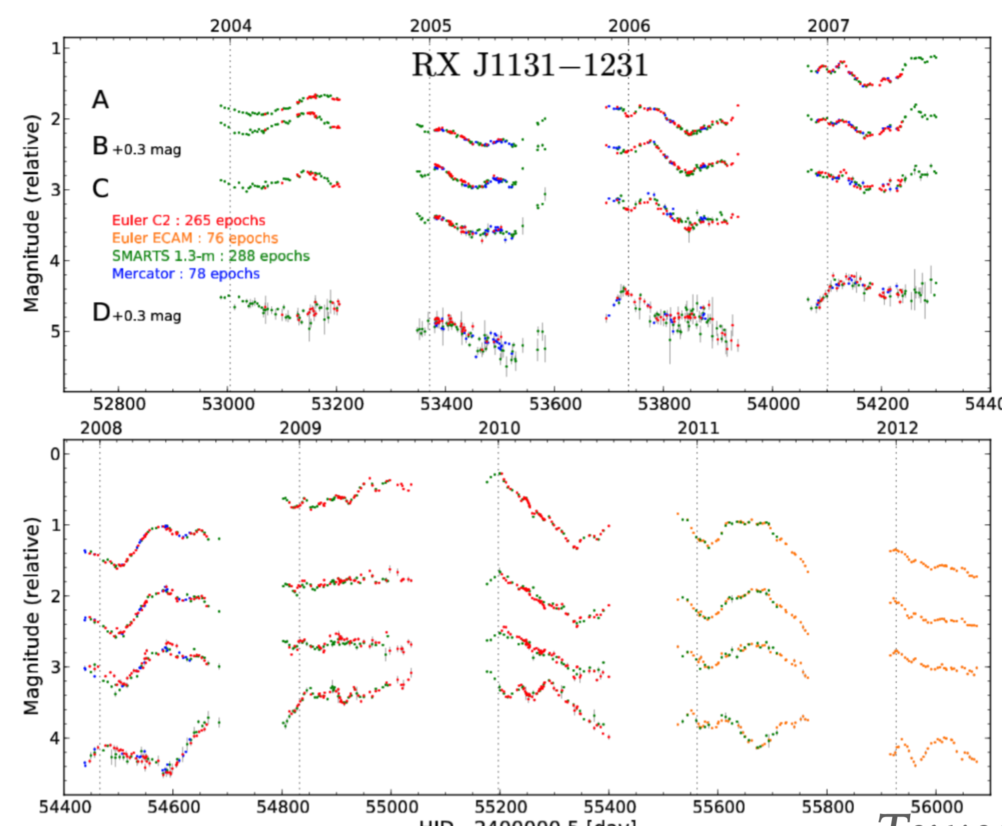

Tewes et al. 2013b

CURRENT CONSTRAINTS ON COSMOLOGY FROM TIME DELAYS

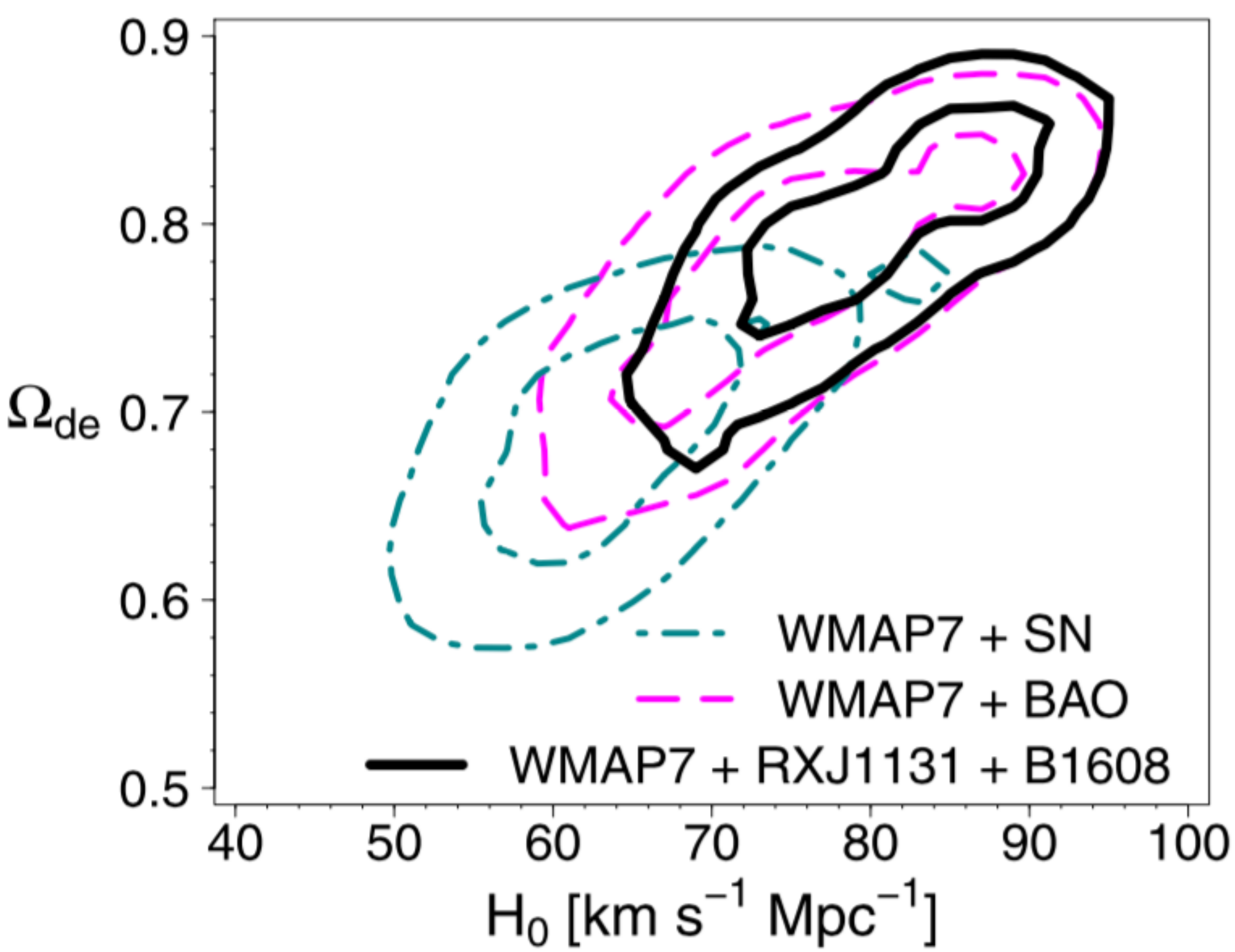

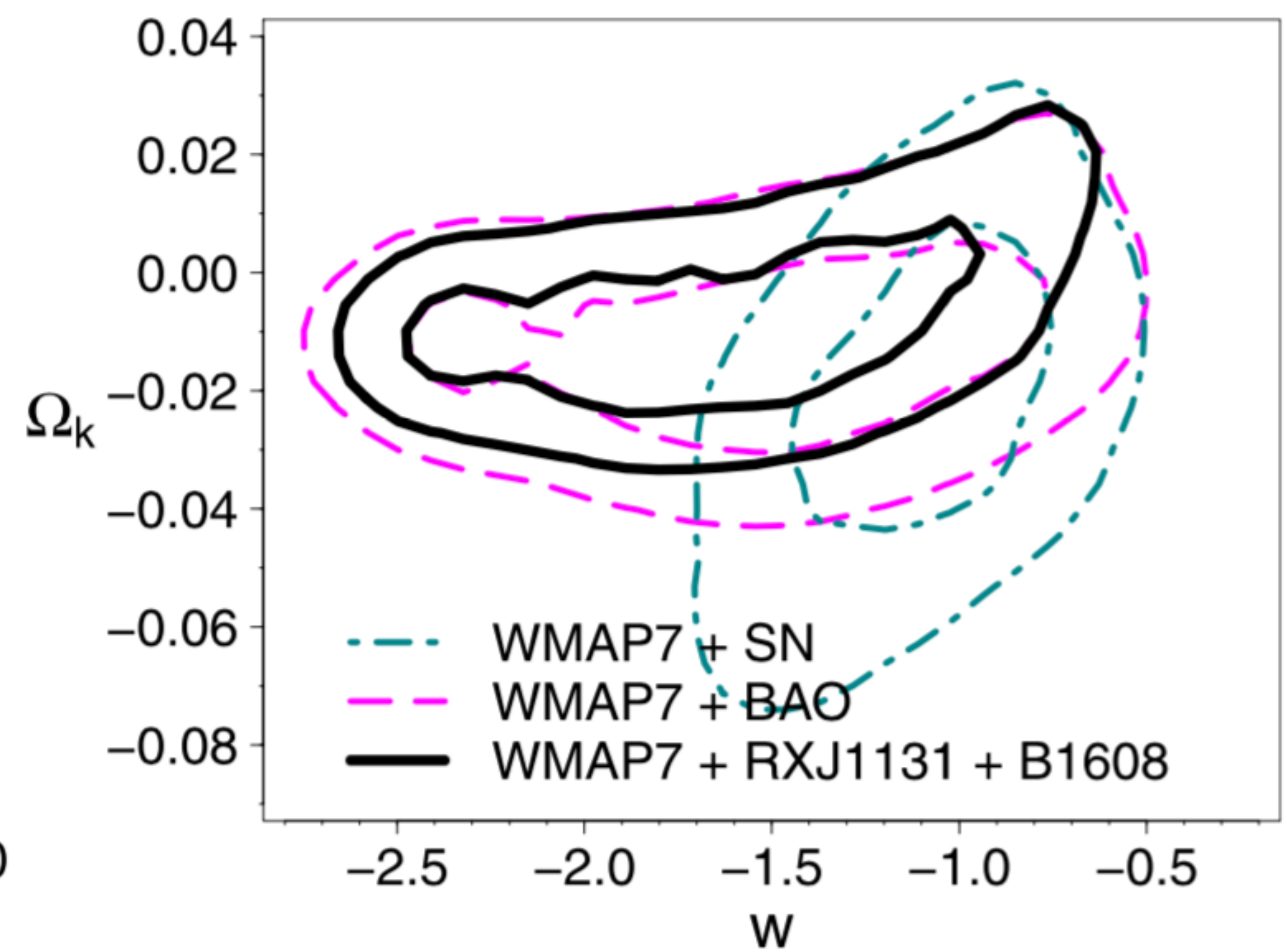

Suyu et al. 2013

Results are going to improve by means of the combination of many lenses (e.g. LSST)

COSMOGRAPHY WITH SOURCES AT MULTIPLE REDSHIFTS

- Even if time delay measurements are not available, the sensitivity to cosmology remains in the astrometric constraints
- With only one lensed source, the distance ratio is degenerate with the mass distribution
- With constraints from multiple sources, one can try to break the degeneracy by measuring the so called "family ratio"
- This technique could be used in the case of e.g. compound lenses, but also in galaxy clusters, where it is easier to observe lensing of many sources

$$\vec{\beta} = \vec{\theta} - \frac{D_{LS}}{D_S}\hat{\vec{\alpha}}(\vec{\theta})$$

depends on cosmology

depends on the mass distr.

$$\Xi_{S1,S2}(\vec{\pi}) = \frac{D_{LS,1}(\vec{\pi})D_{S,2}(\vec{\pi})}{D_{LS,2}(\vec{\pi})D_{S,1}(\vec{\pi})}$$

COSMOGRAPHY: GALAXY CLUSTERS

Mass model with 3 PIEMD potentials; 58 cluster galaxies
Bayesian optimization: 32 constraints, 21 free parameters;
RMS = 0.6 arcsec; 28 multiple images from 12 sources with
spec z, flat Universe prior

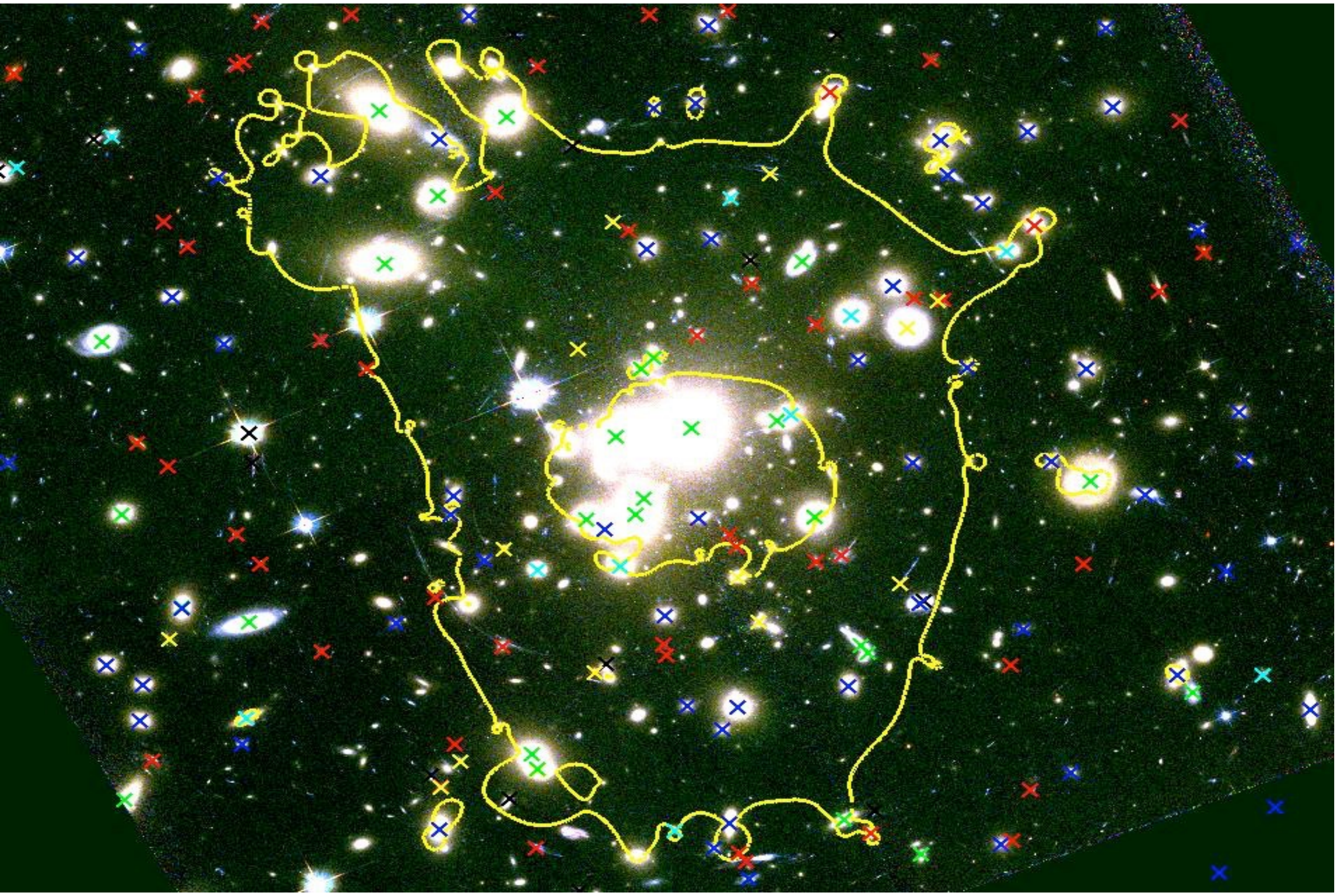

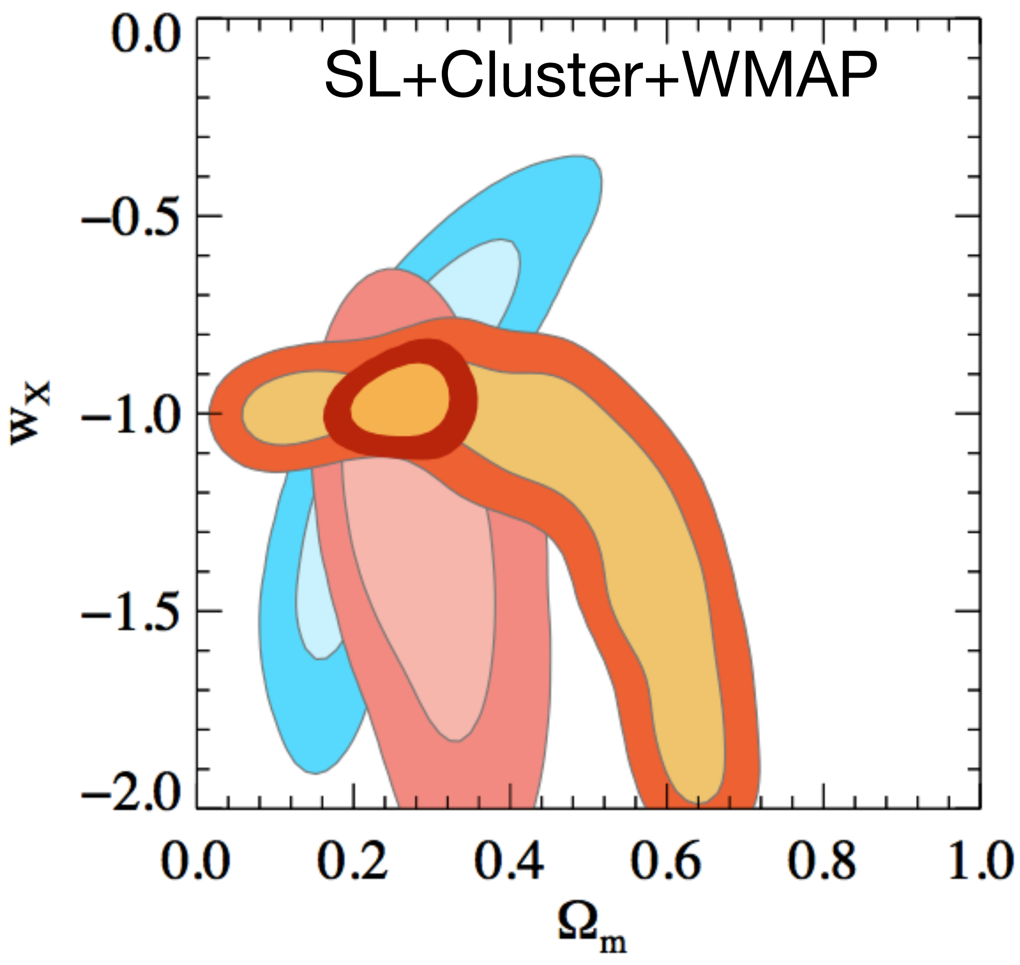

D'Aloisio & Natarajan 10; Jullo & Kneib 09: Jullo+ 10

COSMOGRAPHY: GALAXY CLUSTERS

Caminha et al. 2016

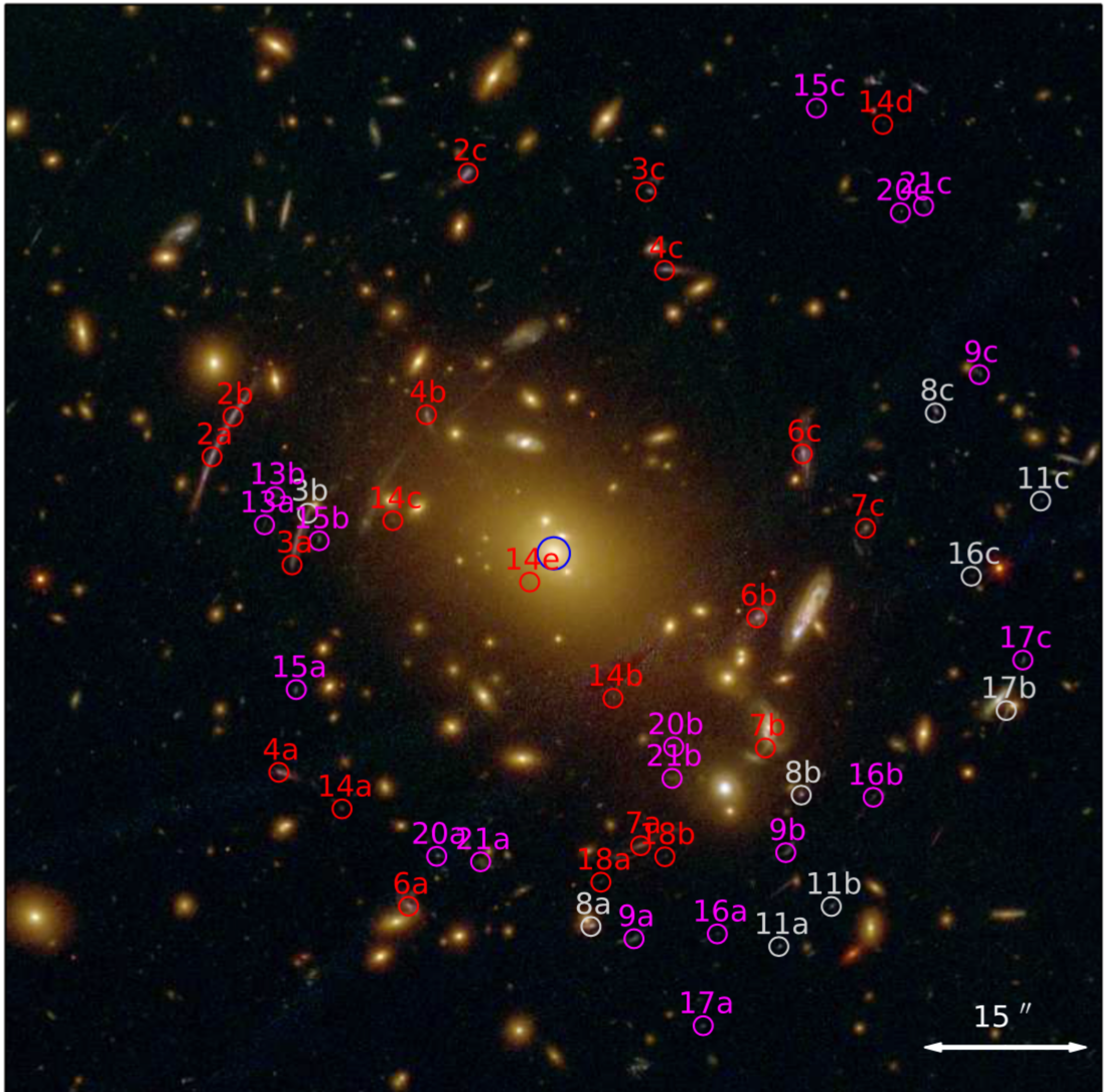

Abell S1063@z=0.348 is one of the FFs.

Spectroscopic follow-up with VIMOS and MUSE @VLT allowed to measure redshifts for 10 families of multiple images (z=1.035-6.111)+confirm the membership of many cluster galaxies.

Very accurate mass modeling, using only secured lensing constraints

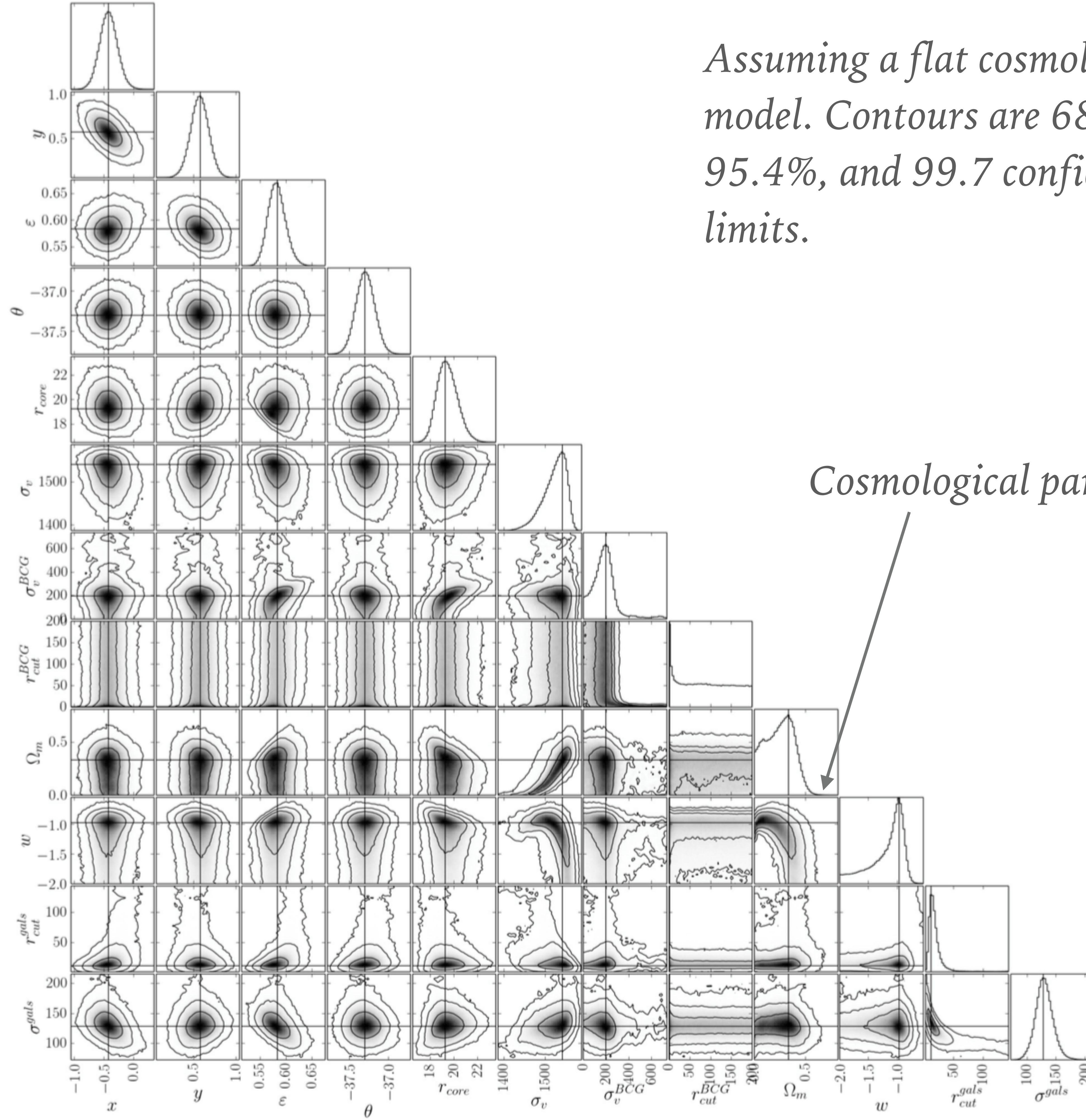

Assuming a flat cosmological model. Contours are 68%, 95.4%, and 99.7 confidence limits.

Cosmological parameters